

---

# **Semiconductor Devices**

## **THIRD EDITION**

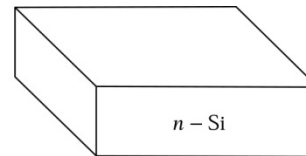
**S. M. Sze and M. K. Lee**

---

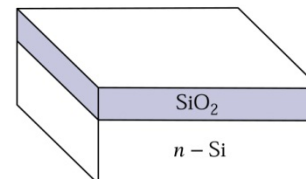
## **Chapter 3**

### ***p–n Junction***

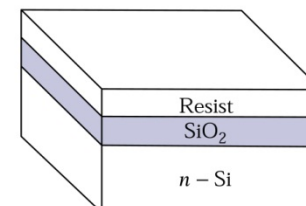
- (a) A bare *n*-type Si wafer. (b) An oxidized Si wafer by dry or wet oxidation.  
(c) Application of resist.  
(d) Resist exposure through the mask.



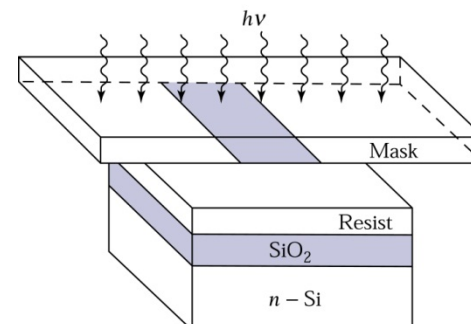
(a)



(b)

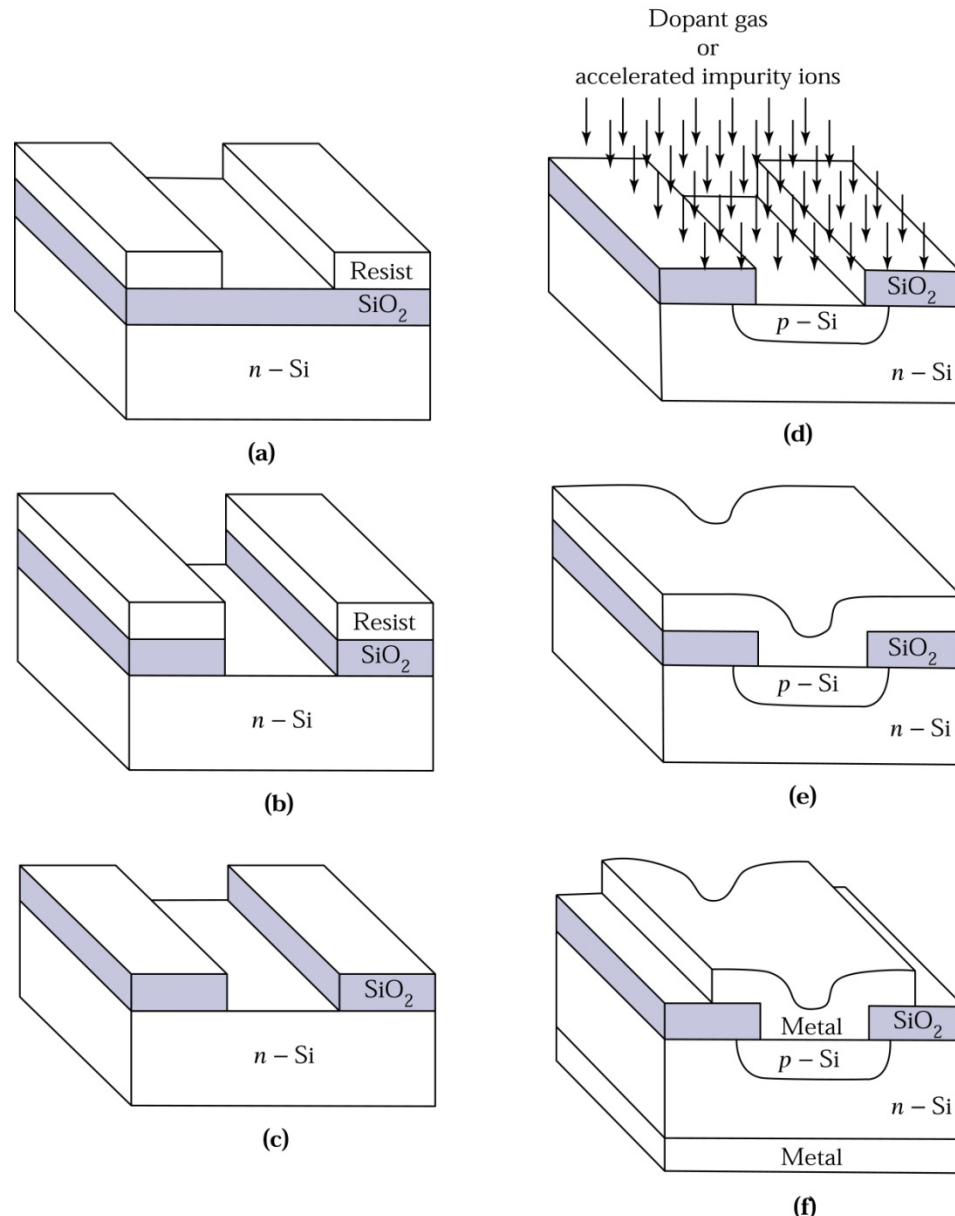


(c)



(d)

- (a) The wafer after the development. (b) The wafer after  $\text{SiO}_2$  removal. (c) The final result after a complete lithography process.
- (d) A  $p-n$  junction is formed in the diffusion or implantation process.
- (e) The wafer after metalization. (f) A  $p-n$  junction after the compete process.



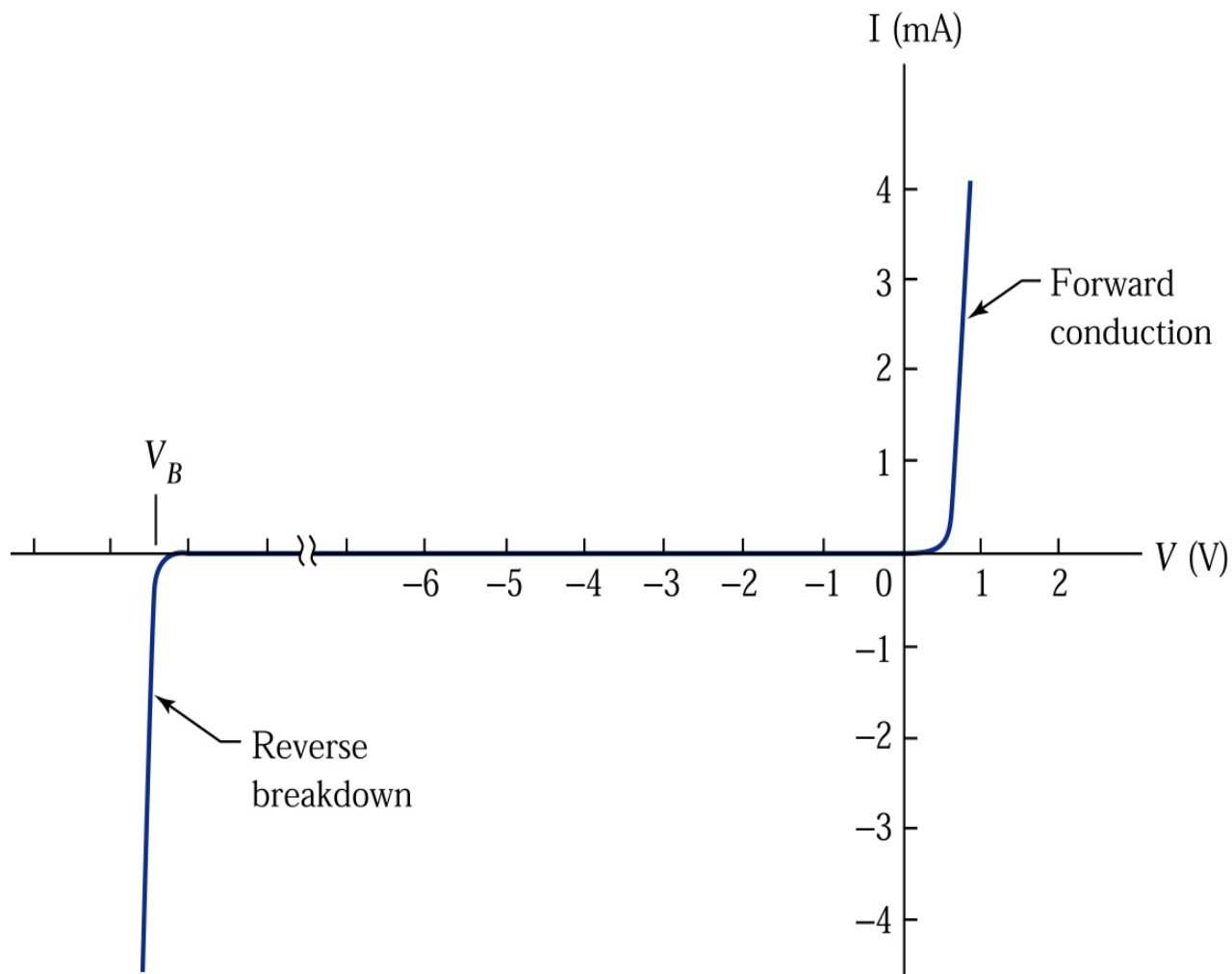
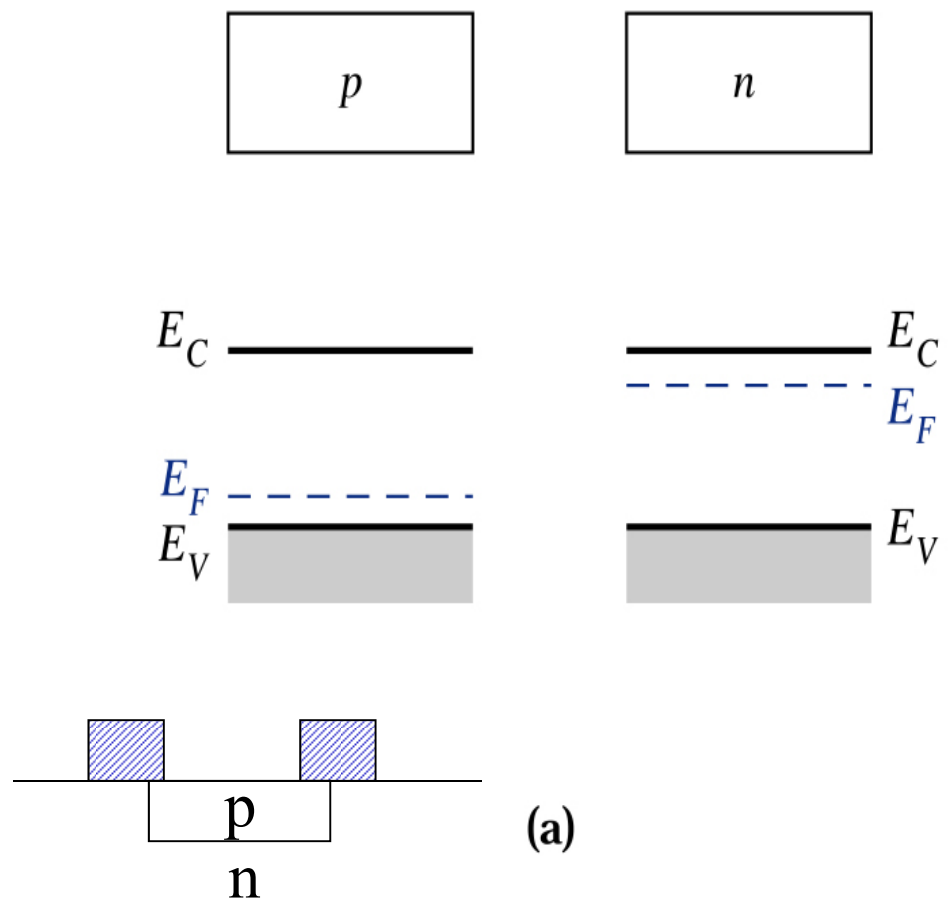
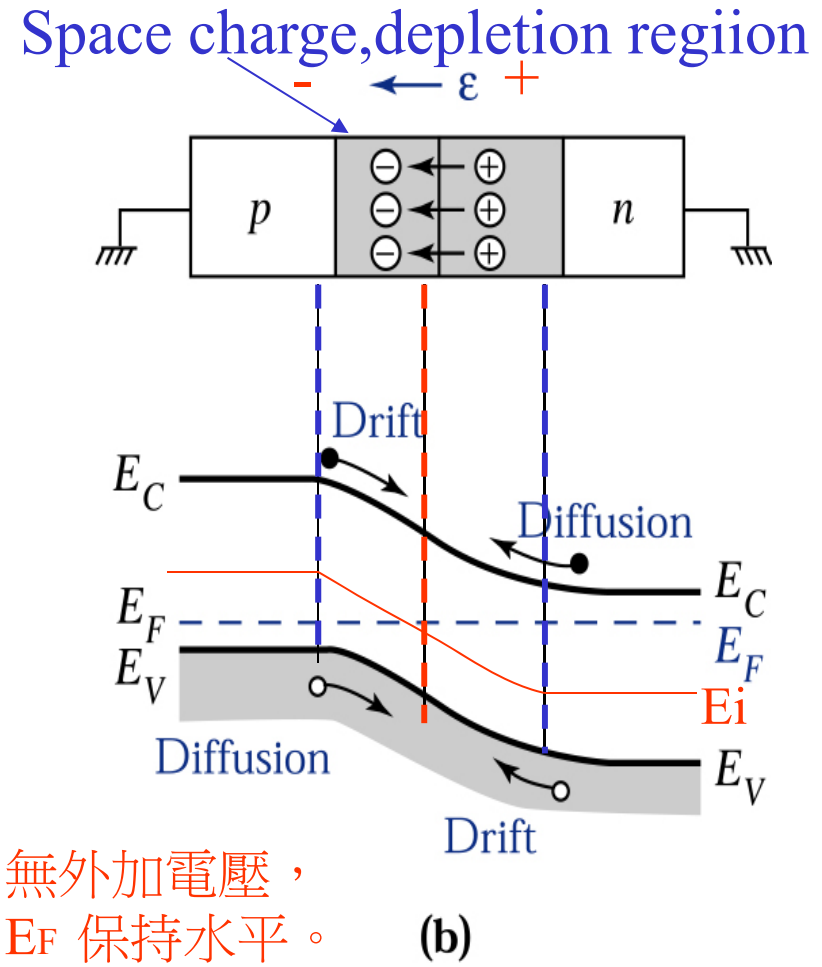


**Figure 3.1** Current-voltage characteristics of a typical silicon  $p-n$  junction.

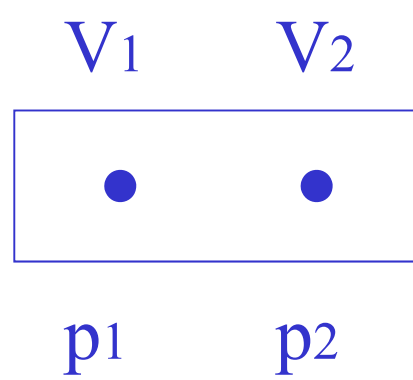


(a)



(b)

**Figure 3.2.** (a) Uniformly doped  $p$ -type and  $n$ -type semiconductors before the junction is formed. (b) The electric field in the depletion region and the energy band diagram of a  $p$ - $n$  junction in thermal equilibrium.



$$\begin{aligned}
 J_p &= J_p(\text{drift}) + J_p(\text{diffusion}) \\
 &= q\mu_p p \mathcal{E} - qD_p \frac{dp}{dx} = 0 \\
 &= q\mu_p p \left( \frac{1}{q} \frac{dE_i}{dx} \right) - kT\mu_p \frac{dp}{dx} = 0,
 \end{aligned} \tag{1}$$

$$\begin{aligned}
 -\mu_p p \frac{dV}{dx} &= D_p \frac{dp}{dx} \\
 dV &= -\frac{D_p}{\mu_p} \times \frac{dp}{p} \\
 V_{21} &= \frac{kT}{q} \ln \frac{p_1}{p_2}
 \end{aligned}$$

又由已知  $p = n_i e^{(E_i - E_F)/kT}$  (2)

微分

$$\frac{dp}{dx} = \frac{p}{kT} \left( \frac{dE_i}{dx} - \frac{dE_F}{dx} \right) \quad (3)$$

(3)代入(1)

$$J_p = \mu_p p \frac{dE_F}{dx} = 0 \quad (4)$$

$$\frac{dE_F}{dx} = 0.$$

(5) (1)無外加電場  
(2)熱平衡

- 注意  $dE_i/dx \neq 0$

- 由Poisson's eq.

$$\nabla^2 V = -\frac{\rho}{\epsilon}$$

$$(\nabla \cdot D = \rho)$$

$$\frac{d\Psi}{dx} = -E$$

$$\frac{d^2\psi}{dx^2} \equiv -\frac{d\epsilon}{dx} = -\frac{\rho_s}{\epsilon_s} = -\frac{q}{\epsilon_s} (N_D - N_A + p - n).$$

正電 負電

(7)

中性區  $\rightarrow \frac{d^2\psi}{dx^2} = 0$  即無  $\rho_s$  無  $E$  (8)

所以  $N_D - N_A + p - n = 0.$  (9)

-  $\psi_p \equiv -\frac{1}{q}(E_i - E_F) \Big|_{x \leq -x_p} = -\frac{kT}{q} \ln\left(\frac{N_A}{n_i}\right).$  (ND=n=0, ρ=NA)  
 p-type

↑  
中性區相對EF之電子電位

+  $\psi_n \equiv -\frac{1}{q}(E_i - E_F) \Big|_{x \geq x_n} = -\frac{kT}{q} \ln\left(\frac{N_D}{n_i}\right).$  (NA=p=0, ρ=ND)  
 n-type



$$V_{bi} = \psi_n - \psi_p = \frac{kT}{q} \ln \left( \frac{N_A N_D}{n_i^2} \right).$$

$$= \frac{kT}{q} \ln \frac{n_{n0}}{n_{p0}} \quad (12)$$

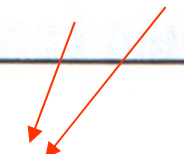
Built in potential

$$\frac{\frac{n_{n0}}{n_i^2}}{\frac{n_{n0}}{n_{p0}}} \Rightarrow n_{n0} = n_{p0} e^{\frac{qV_{bi}}{kT}}$$
$$P_{p0}$$

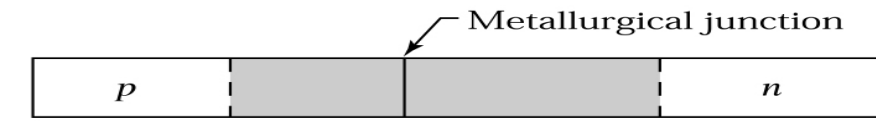
空乏區中，Poisson's eq. 為

$$\frac{d^2\psi}{dx^2} = \frac{q}{\epsilon_s} (N_A - N_D). \quad (13)$$

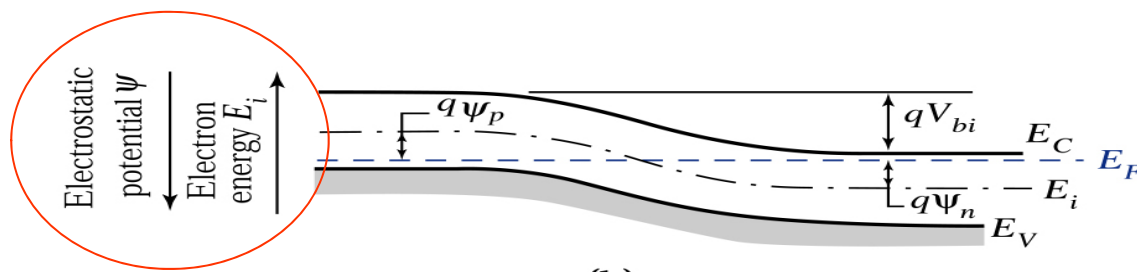
$$\frac{d^2\psi}{dx^2} \equiv -\frac{d\mathcal{E}}{dx} = -\frac{\rho_s}{\epsilon_s} = -\frac{q}{\epsilon_s} (N_D - N_A + p - n). \quad (7)$$



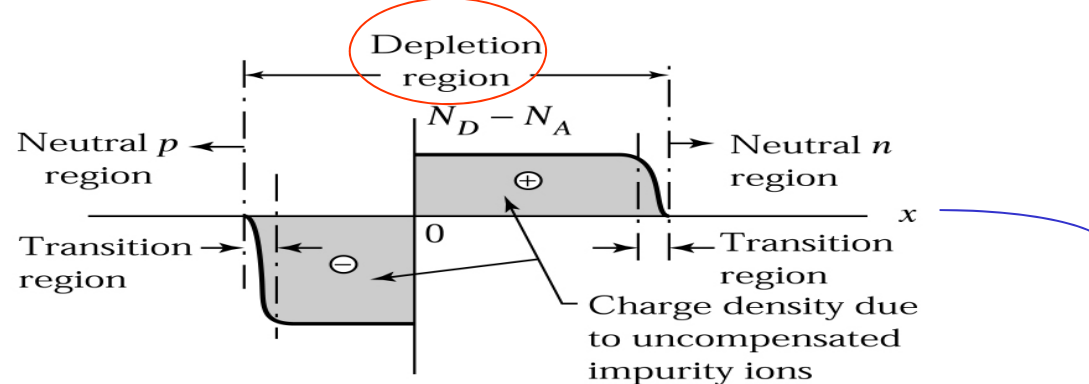
0



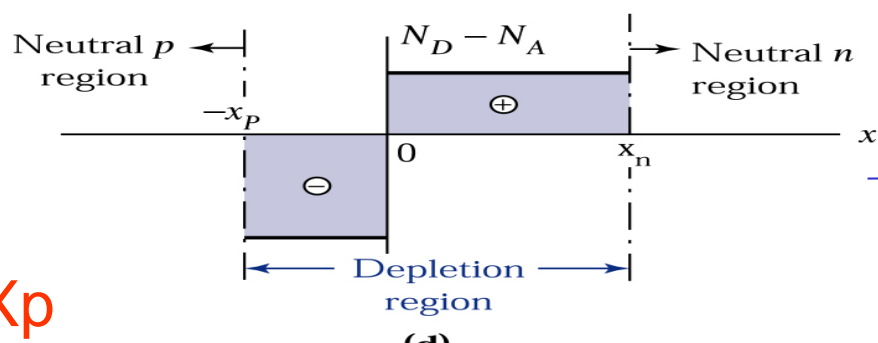
(a)



(b)



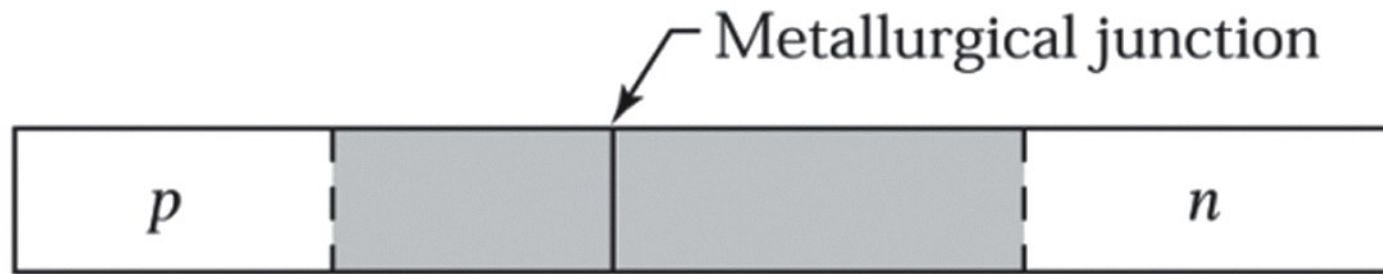
(c)



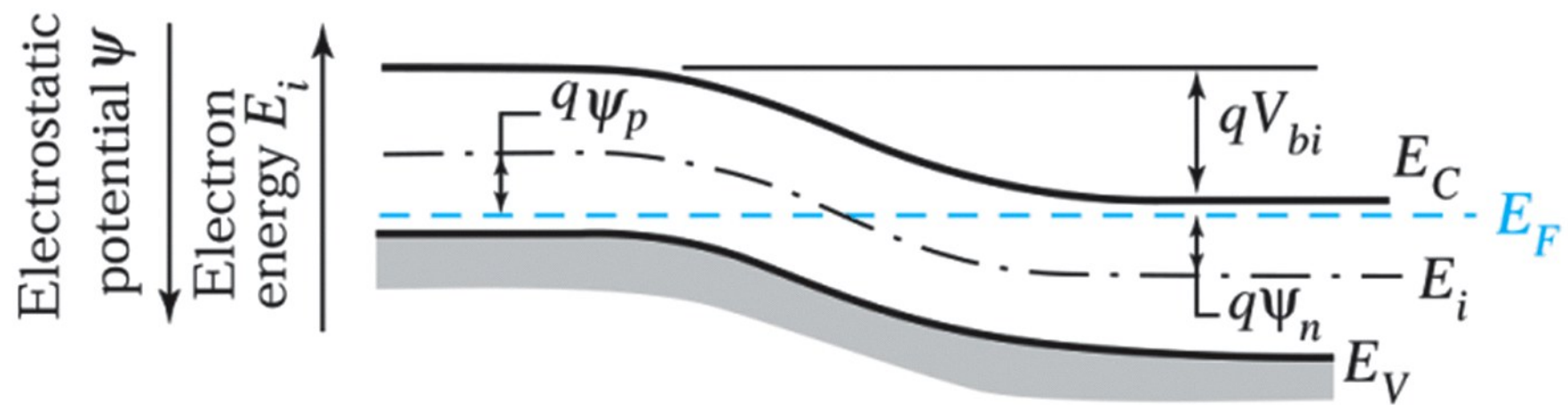
(d)

$$N_D \cdot X_n = N_A \cdot X_p$$

Figure 3.3

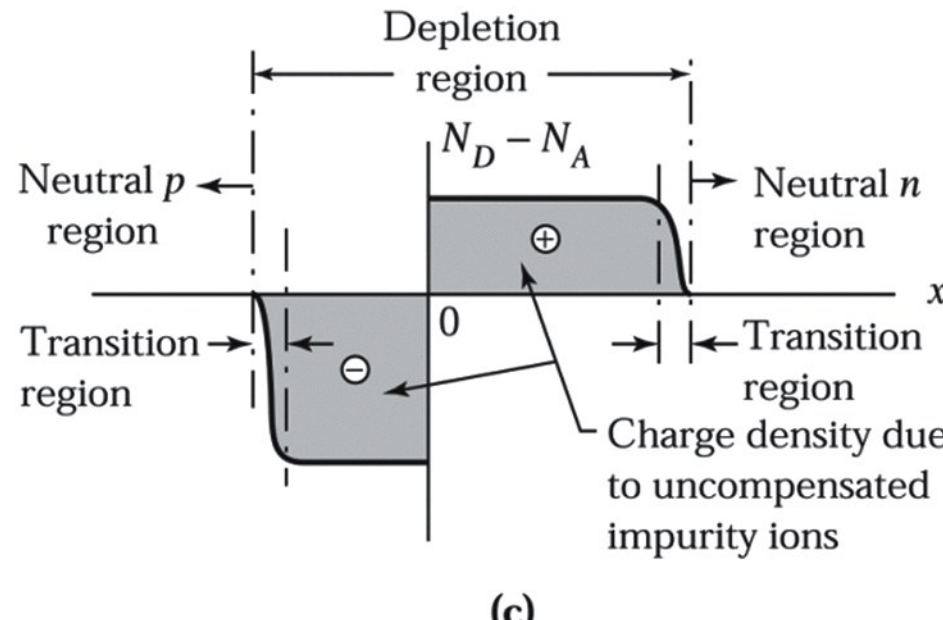


(a)

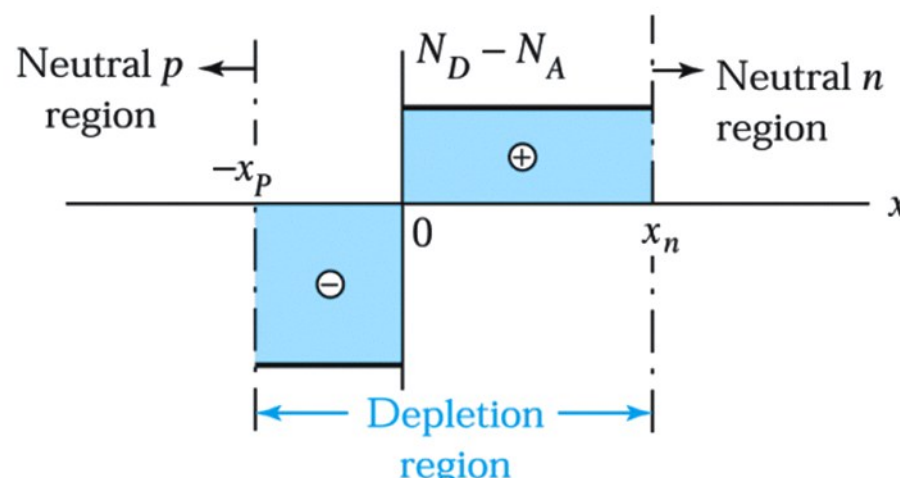


(b)

**Figure 3.3ab**  
© John Wiley & Sons, Inc. All rights reserved.



(c)



(d)

Figure 3.3cd  
© John Wiley & Sons, Inc. All rights reserved.

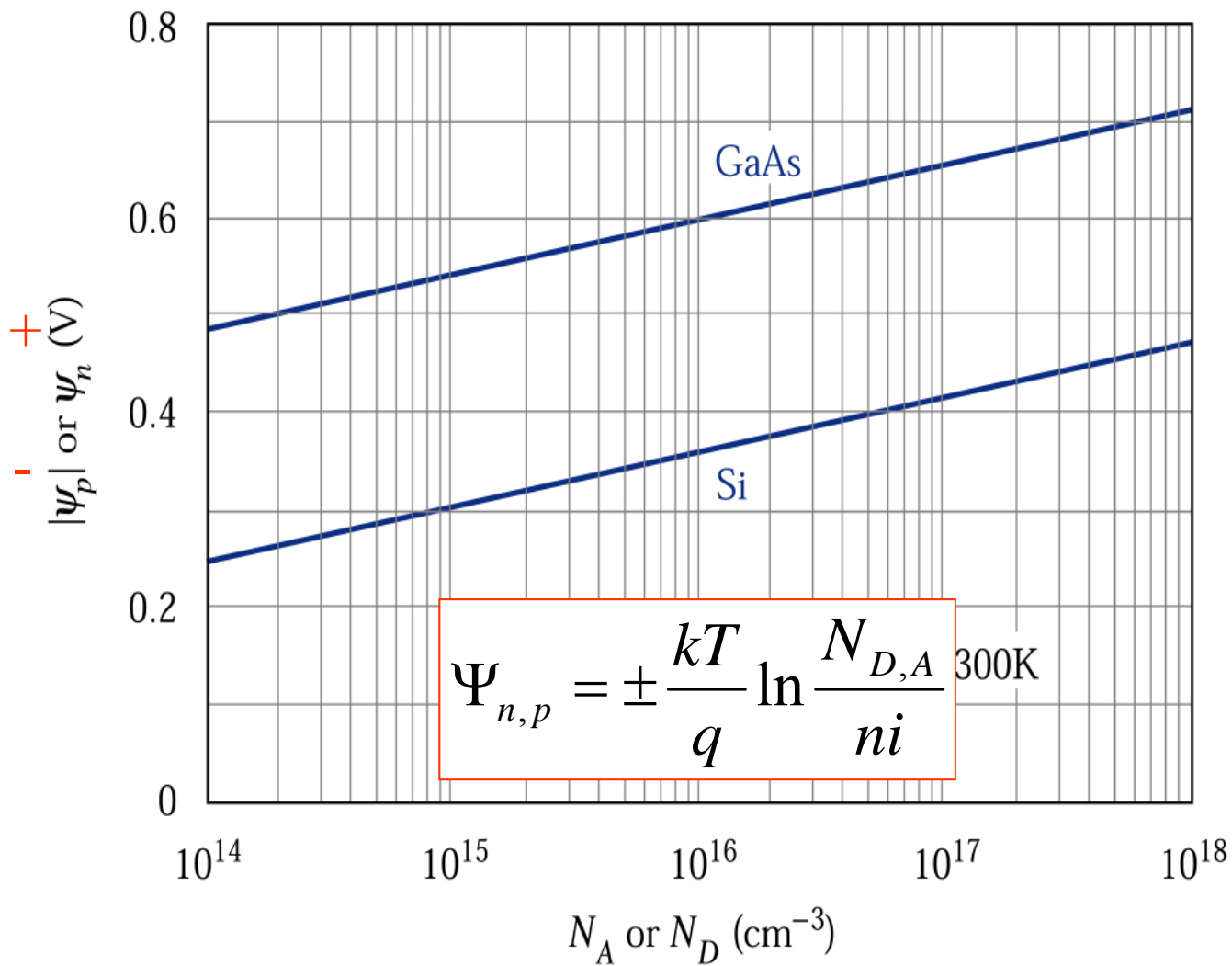


**Figure 3.4.** Built-in potentials on the *p*-side and *n*-side of abrupt junctions in Si and GaAs as a function of impurity concentration.

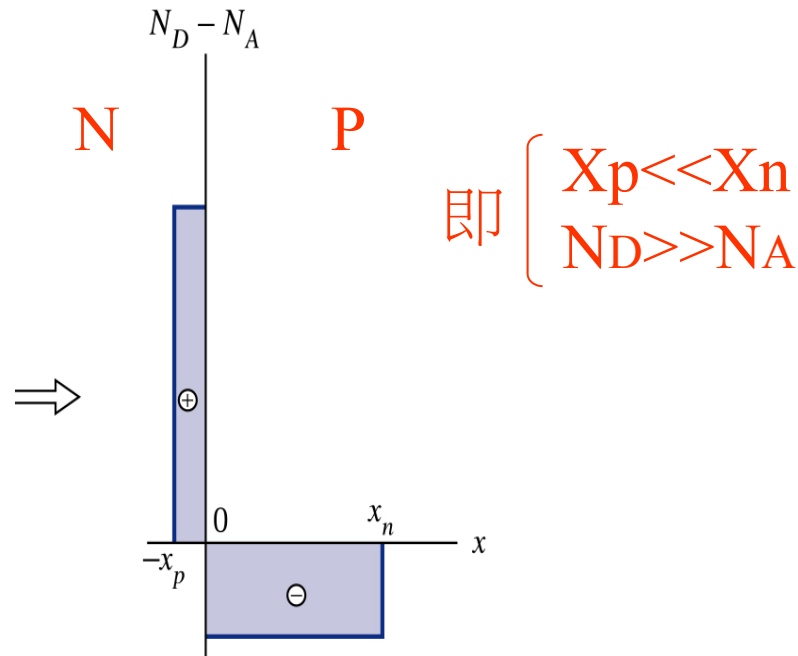
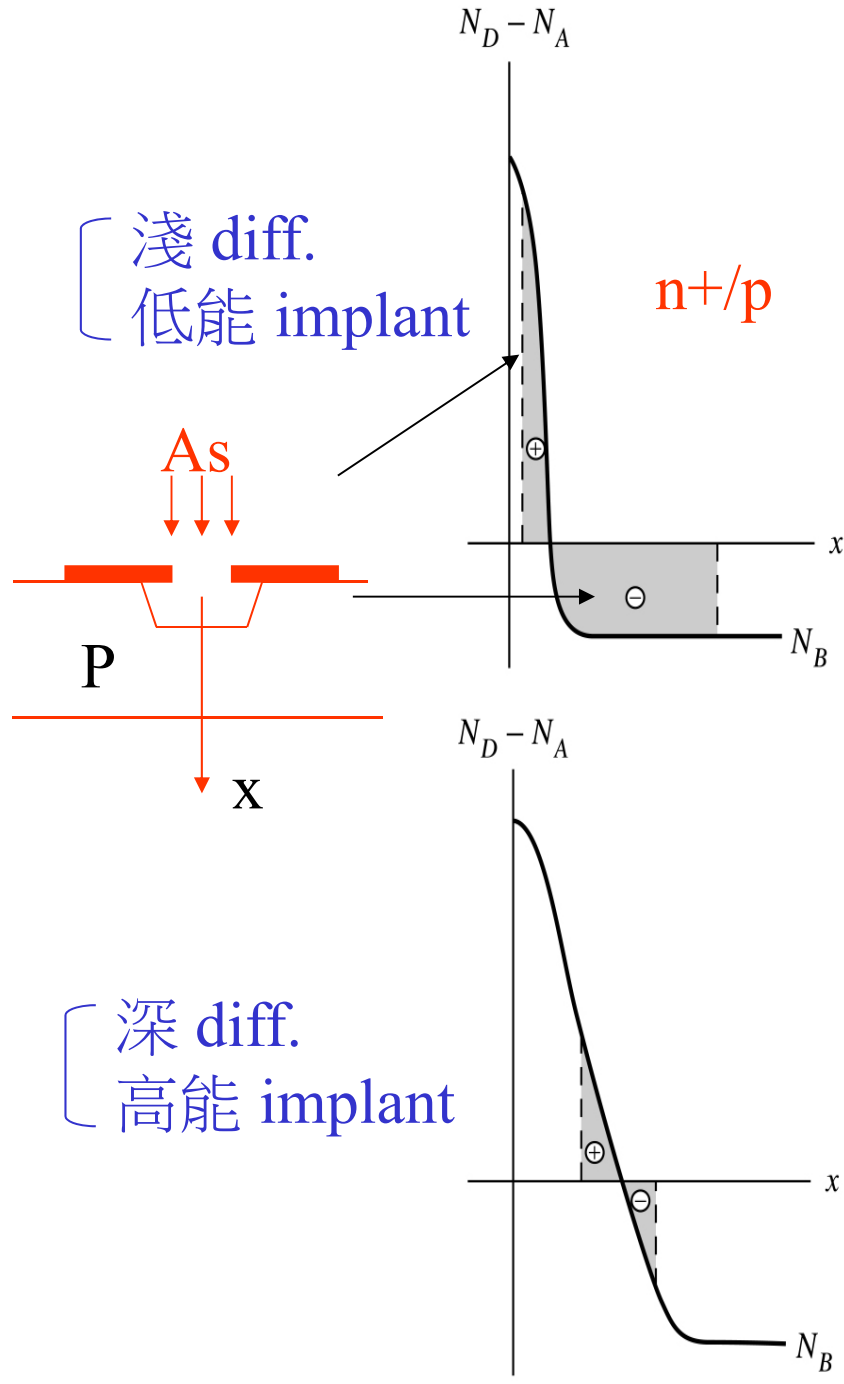
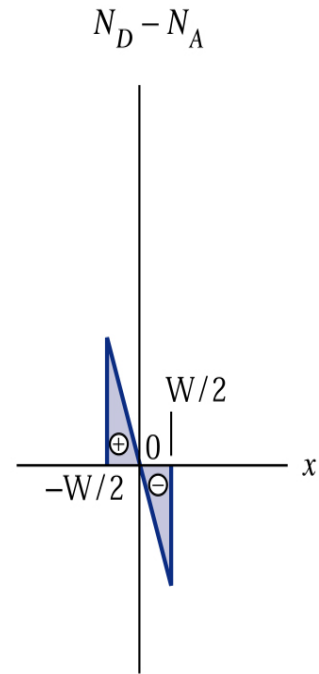


**Figure 3.5.**  
 Approximate doping profiles.  
 (a) **Abrupt** junction.  
 (b) Linearly graded junction.



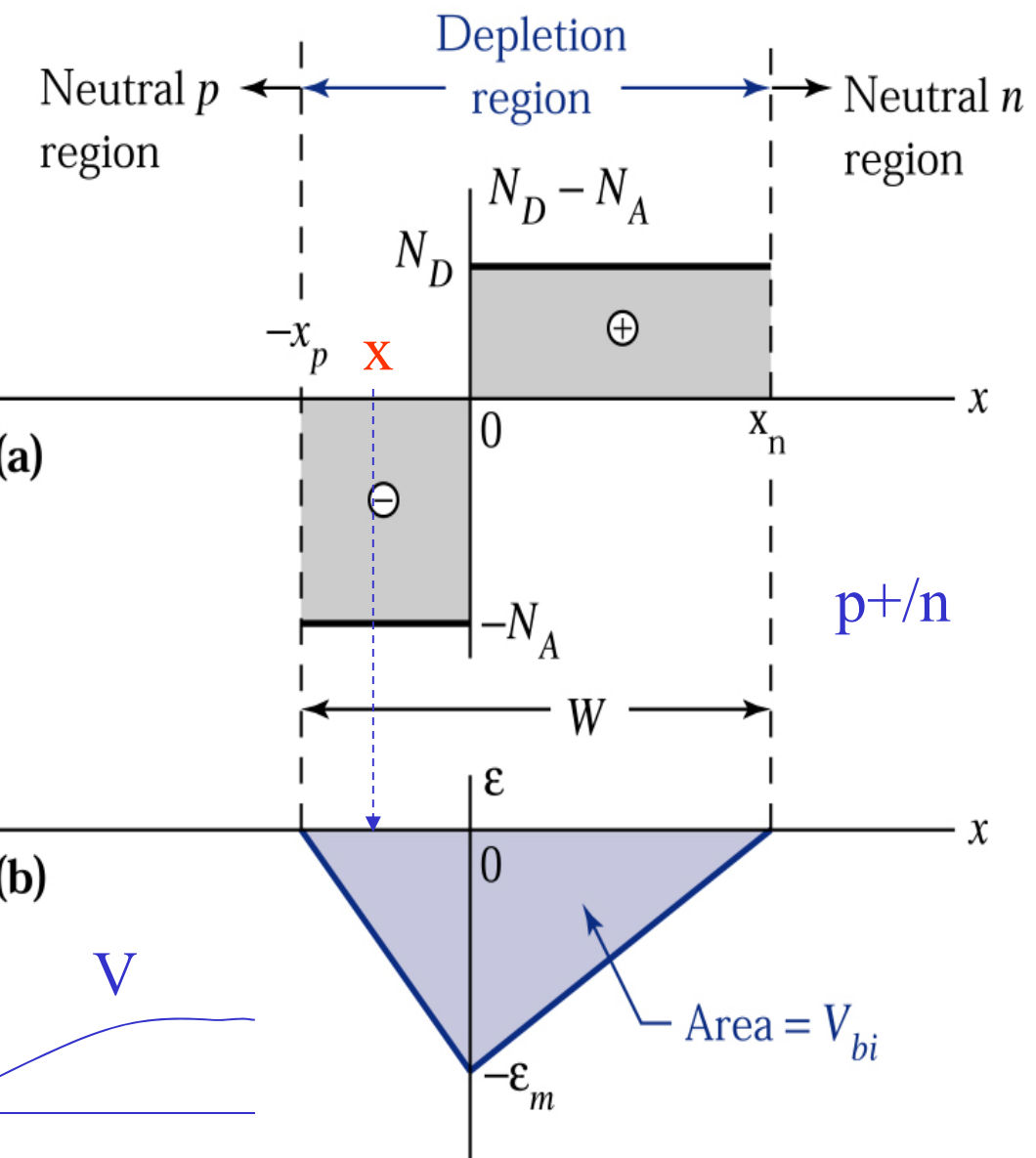
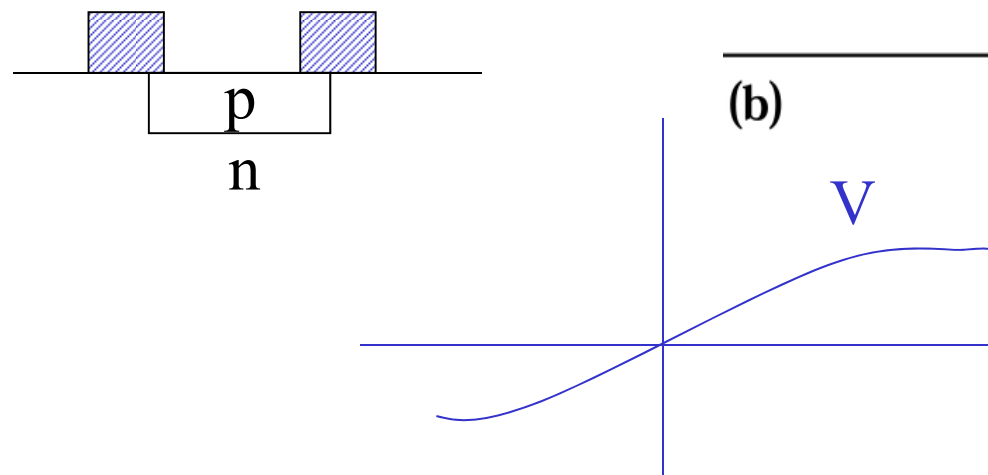
# Abrupt Junction

計算方便，亦大都屬於此種Junction

$$\left\{ \begin{array}{l} \frac{d^2\psi}{dx^2} = +\frac{qN_A}{\epsilon_s} \quad \text{for } -x_p \leq x < 0, \\ \frac{d^2\psi}{dx^2} = -\frac{qN_D}{\epsilon_s} \quad \text{for } 0 < x \leq x_n. \end{array} \right. \quad (14a)$$

**Figure 3.6.**

(a) Space charge distribution in the depletion region at thermal equilibrium. (b) Electric-field distribution. The shaded area corresponds to the built-in potential.



$$\left\{ \begin{array}{l} N_A x_p = N_D x_n. \\ W = x_p + x_n. \end{array} \right. \quad \begin{array}{l} (15) \\ (16) \end{array} \quad \begin{array}{l} \text{電中性} \\ \text{Depletion width} \end{array}$$

$$\left\{ \begin{array}{l} \mathcal{E}(x) = -\frac{d\psi}{dx} = -\frac{qN_A(x + x_p)}{\epsilon_s} \quad \text{for } -x_p \leq x < 0 \\ \therefore \frac{d^2\psi}{dx^2} = \frac{qN}{\epsilon_s} \end{array} \right. \quad (17a)$$

$$\left\{ \begin{array}{l} \mathcal{E}(x) = -\mathcal{E}_m + \frac{qN_D x}{\epsilon_x} = \frac{qN_D}{\epsilon_s} (x - x_n) \quad \text{for } 0 < x \leq x_n, \end{array} \right. \quad (17b)$$

$$\mathcal{E}_m = \frac{qN_D x_n}{\epsilon_s} = \frac{qN_A x_p}{\epsilon_s}. \quad (18)$$

area

$$V_{bi} = - \int_{-x_p}^{x_n} \mathcal{E}(x) dx = - \left[ \int_{-x_p}^0 \mathcal{E}(x) dx \right]_{p\text{-side}} - \left[ \int_0^{x_n} \mathcal{E}(x) dx \right]_{n\text{-side}}$$

$$= \frac{qN_A x_p^2}{2\epsilon_s} + \frac{qN_D x_n^2}{2\epsilon_s} = \frac{1}{2} \mathcal{E}_m W. \quad (19)$$

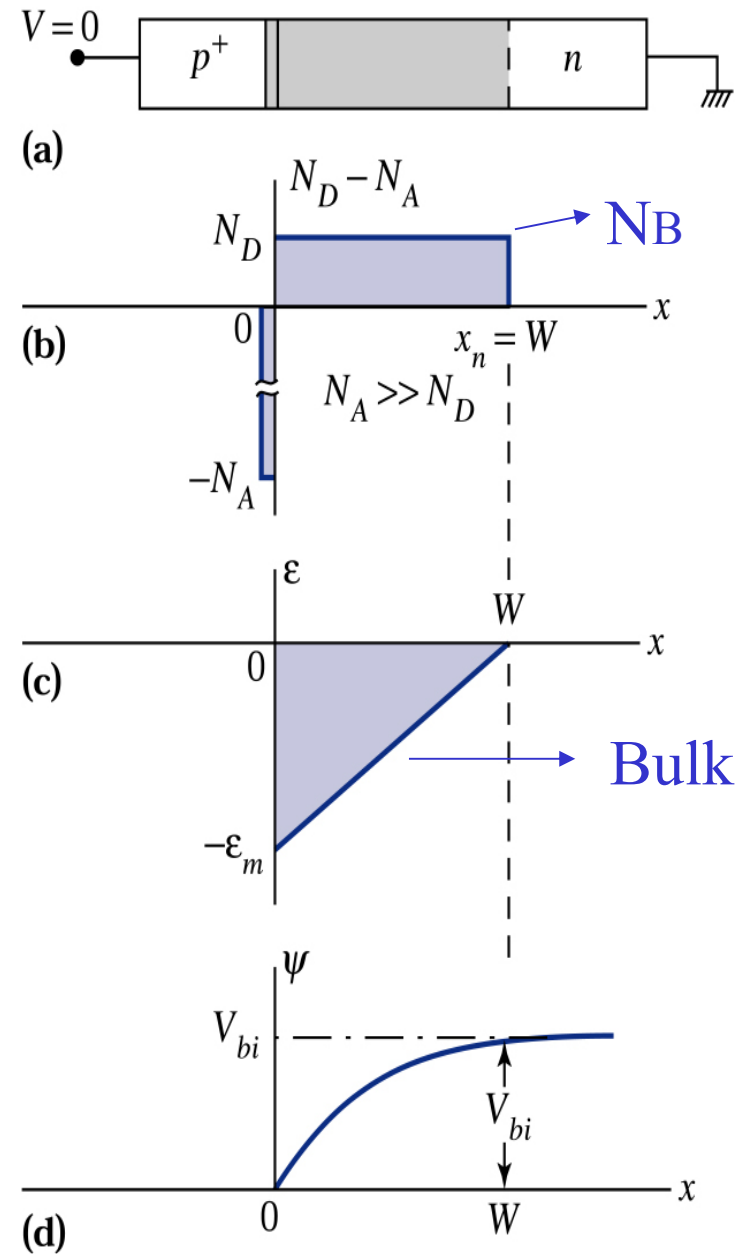
由(15)(19)

$$W = \sqrt{\frac{2\epsilon_s}{q} \left( \frac{N_A + N_D}{N_A N_D} \right)} V_{bi}. \quad (20)$$

**Figure 3.7.**

- (a) One-sided abrupt junction (with  $N_A \gg N_D$ ) in thermal equilibrium.  
(b) Space charge distribution.  
(c) Electric-field distribution.  
(d) Potential distribution with distance, where  $V_{bi}$  is the built-in potential.

p+/n



p+/n  $N_A \gg N_D \rightarrow$

$$W \cong x_n = \sqrt{\frac{2\epsilon_s V_{bi}}{qN_D}}. \quad (21)$$

• 實際p/n junction亦多為abrupt

$$\mathcal{E}_m = \frac{qN_B W}{\epsilon_s} \quad (23)$$

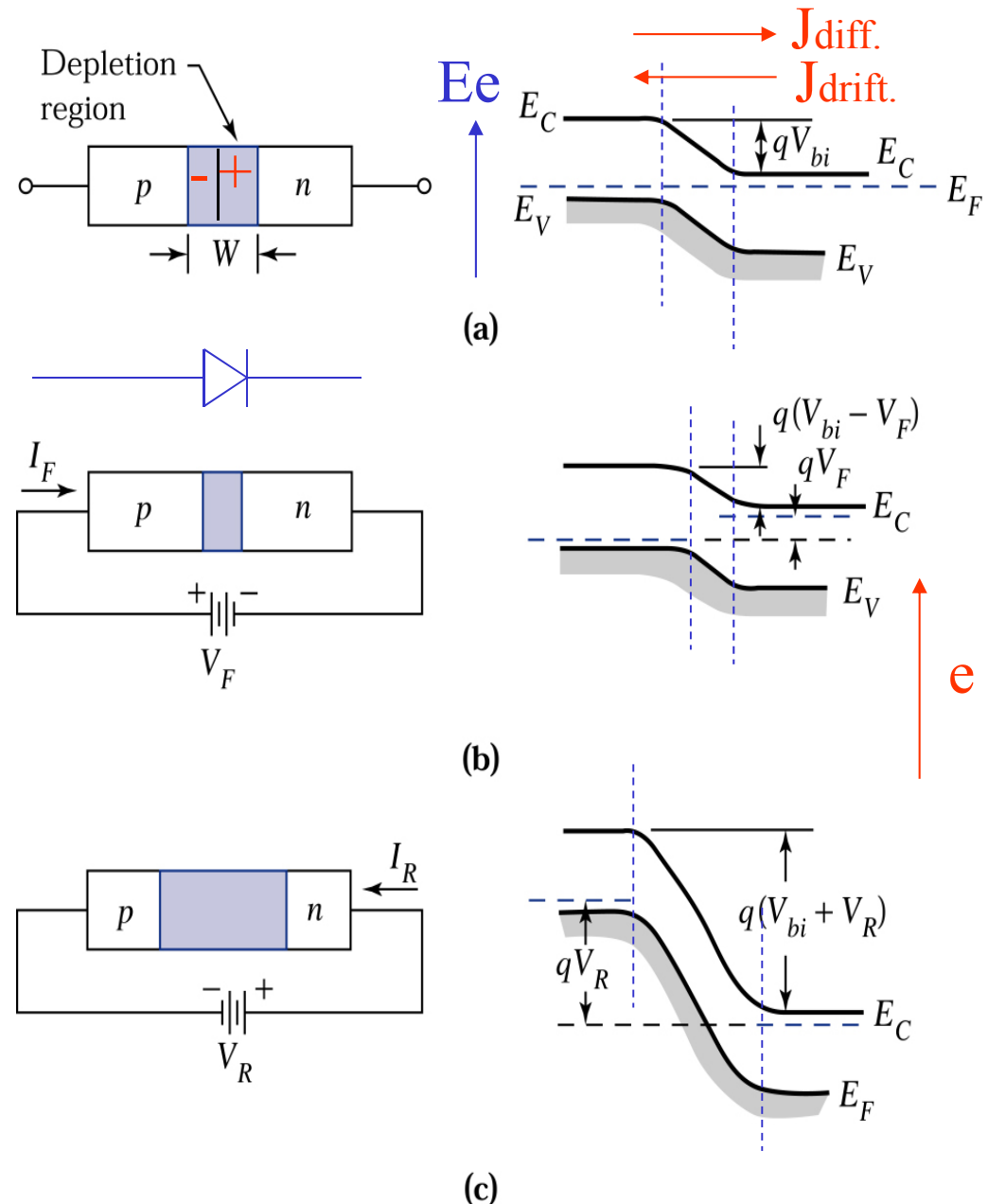
$$\mathcal{E}(x) = \frac{qN_B}{\epsilon_s} \left( -W + x \right) = -\mathcal{E}_m \left( 1 - \frac{x}{W} \right), \quad (24)$$

$$\psi(x) = \frac{V_{bi}x}{W} \left( 2 - \frac{x}{W} \right). \quad (x=W, \Psi(W)=V_{bi}) \quad (26)$$

**Figure 3.8.**

Schematic representation of depletion layer width and energy band diagrams of a *p-n* junction under various biasing conditions.

- a) Thermal-equilibrium condition.
- (b) Forward-bias condition.
- (c) Reverse-bias condition.



•若外加偏壓

$$W = \sqrt{\frac{2\varepsilon_s(V_{bi} - V)}{qN_B}}, \quad (27)$$

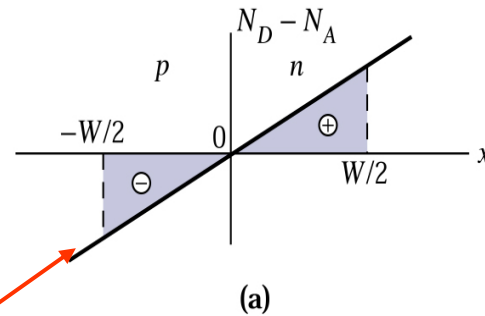
☆ V:forward為正，reverse為負

**Figure 3.9.**

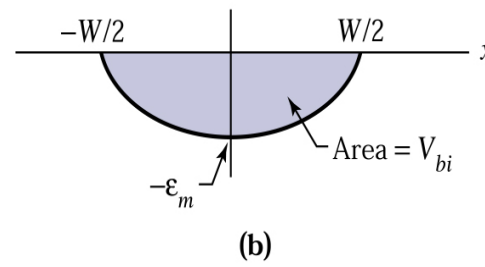
Linearly graded junction in thermal equilibrium.

- (a) Impurity distribution.
- (b) Electric-field distribution.
- (c) Potential distribution with distance.
- (d) Energy band diagram.

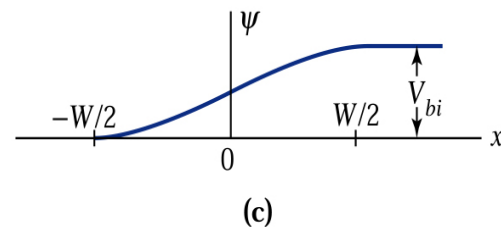
Slope= a



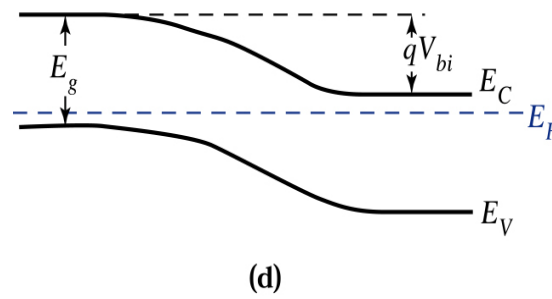
(a)



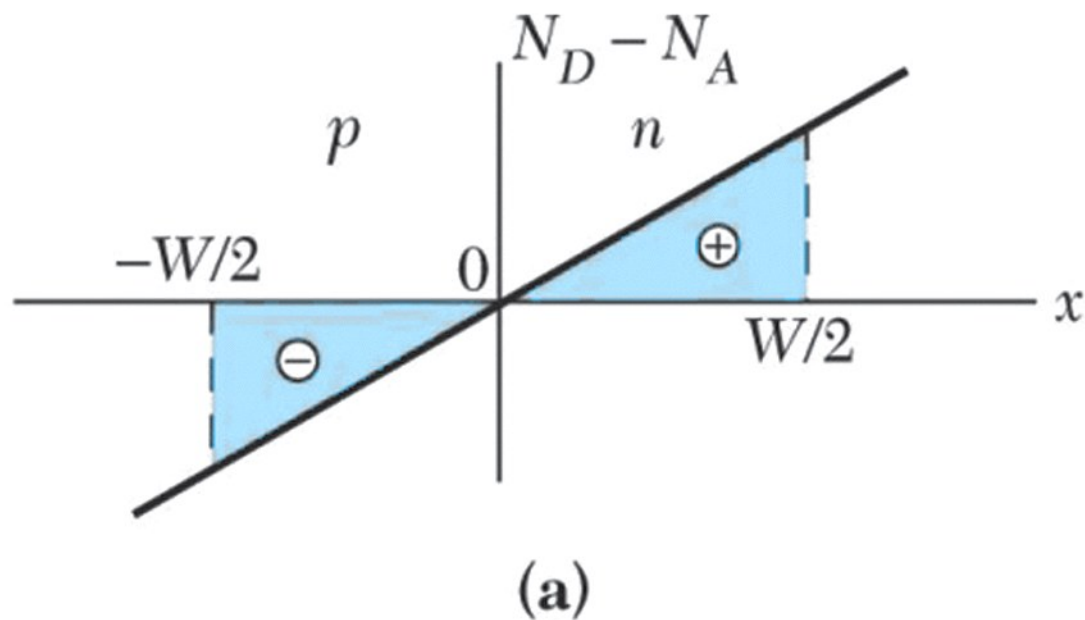
(b)



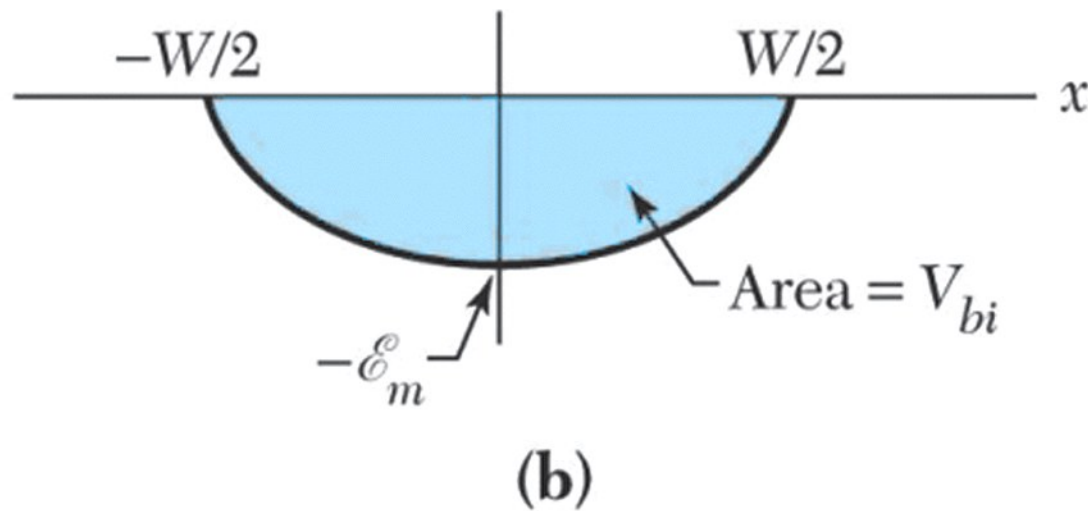
(c)



(d)

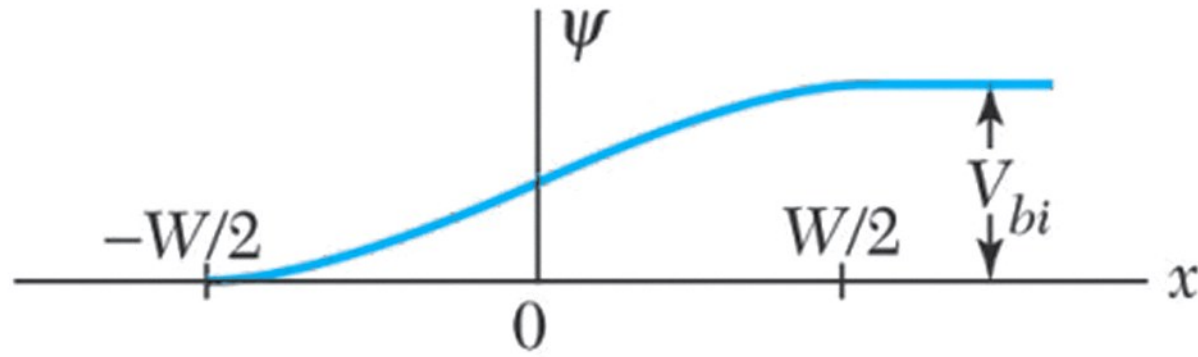


(a)

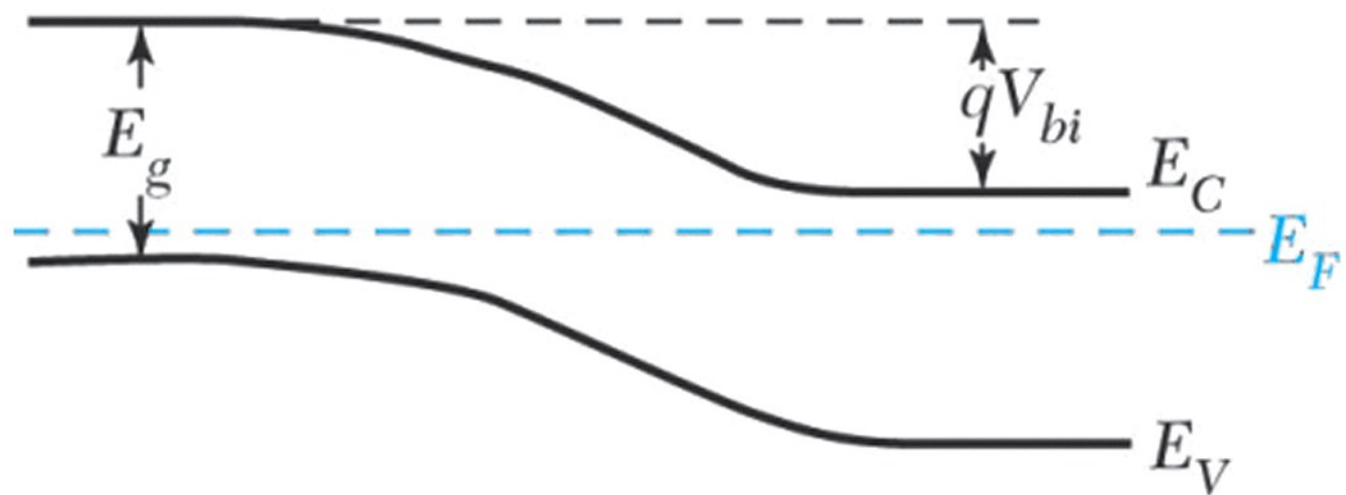


(b)

**Figure 3.9ab**  
© John Wiley & Sons, Inc. All rights reserved.



(c)



(d)

Figure 3.9cd  
© John Wiley & Sons, Inc. All rights reserved.

- Linearly Graded Junction

$$\frac{d^2\psi}{dx^2} = \frac{-d\mathcal{E}}{dx} = \frac{-\rho_s}{\epsilon_s} = \frac{-q}{\epsilon_s} ax \quad -\frac{W}{2} \leq x \leq \frac{W}{2}, \quad (28)$$

$$\mathcal{E}(x) = -\frac{qa}{\epsilon_s} \left[ \frac{(W/2)^2 - x^2}{2} \right]. \quad (29)$$

$$\mathcal{E}_m = \frac{qaW^2}{8\epsilon_s}. \quad (29a)$$

$$W = \left( \frac{12\epsilon_s V_{bi}}{qa} \right)^{1/3}. \quad (31)$$

$V_{bi}$  正比  $\ln(a)$

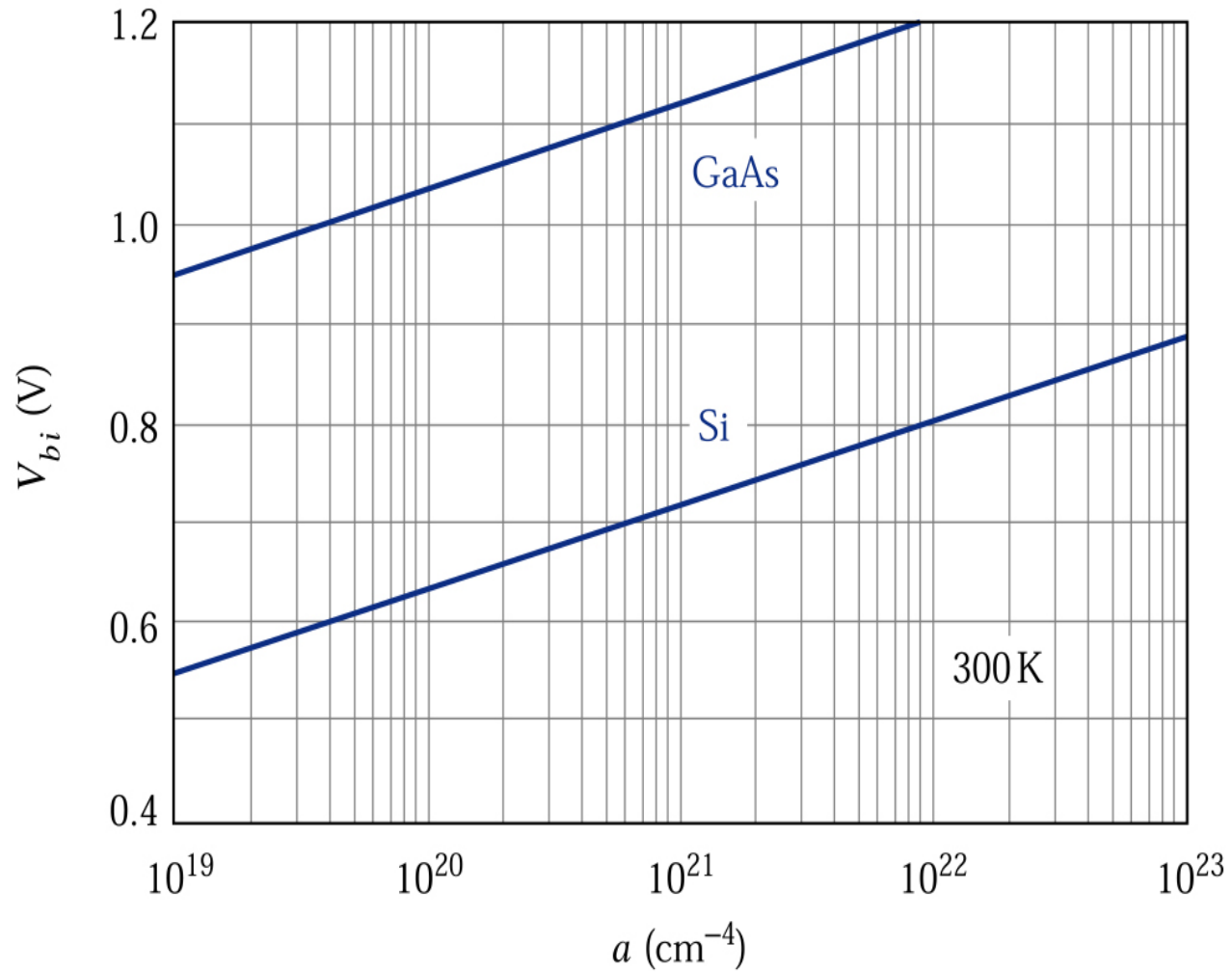


**Figure 3.10.** Built-in potential for a linearly graded junction in Si and GaAs as a function of impurity gradient.

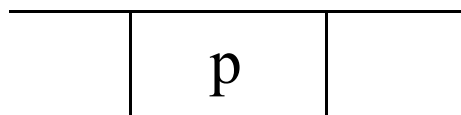
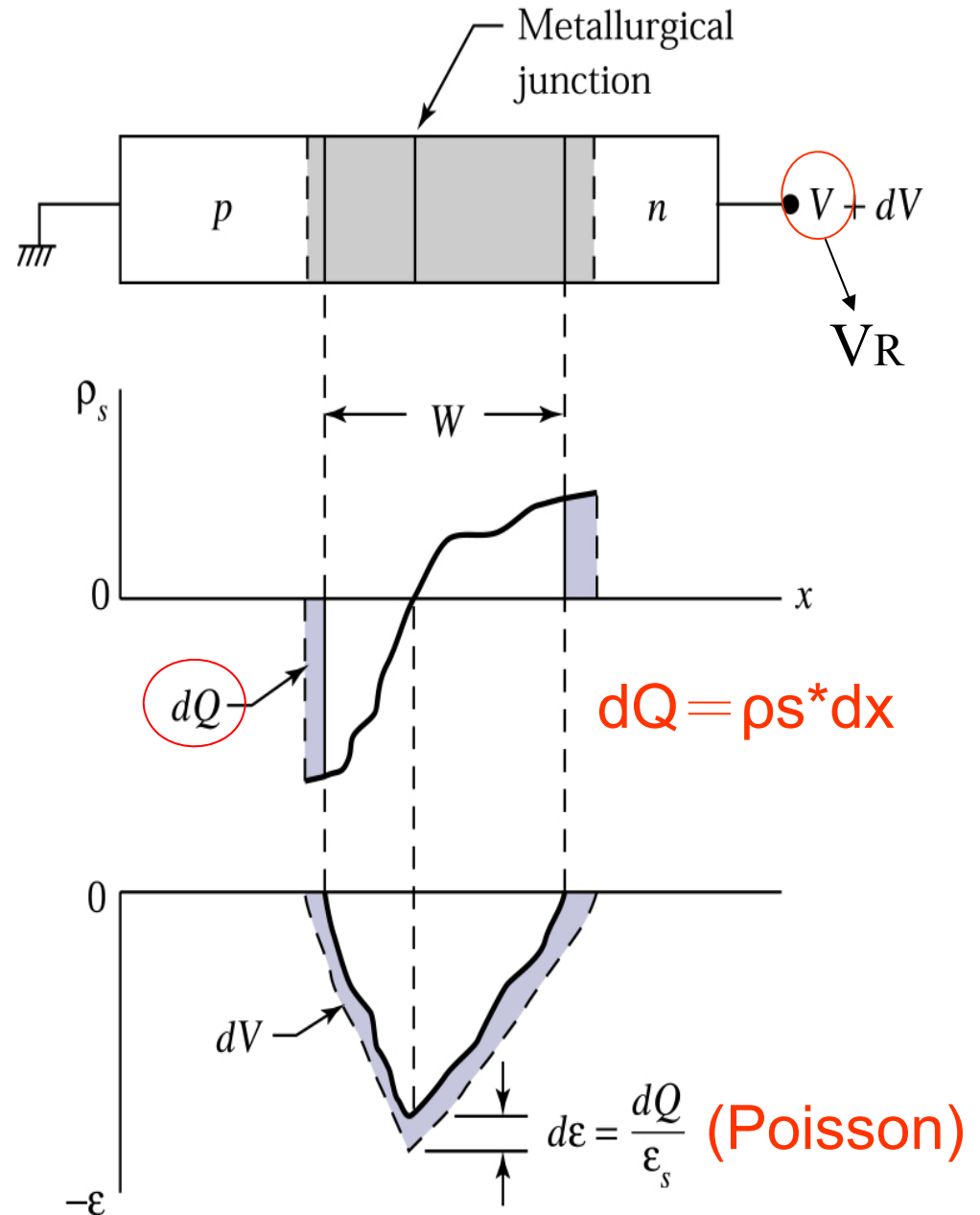


**Figure 3.11.**

(a)  $p$ - $n$  junction with an arbitrary impurity profile under reverse bias. (b) Change in space charge distribution due to change in applied bias. (c) Corresponding change in electric-field distribution.

$$C_j \equiv \frac{dQ}{dV} = -\frac{dQ}{W \frac{dQ}{\epsilon_s}} = \frac{\epsilon_s}{W} \quad (32)$$



For a one-sided abrupt junction

$$C_j = \frac{\epsilon_s}{W} = \sqrt{\frac{q\epsilon_s N_B}{2(V_{bi} - V)}}$$

$$\frac{1}{C_j^2} = \frac{2(V_{bi} - V)}{q\epsilon_s N_B}$$

\*  $1/Cj^2$  vs  $V$  得到一直線

1: 斜率可算  $N_B$  (bulk concentration)

2: 交點可算  $V_{bi}$

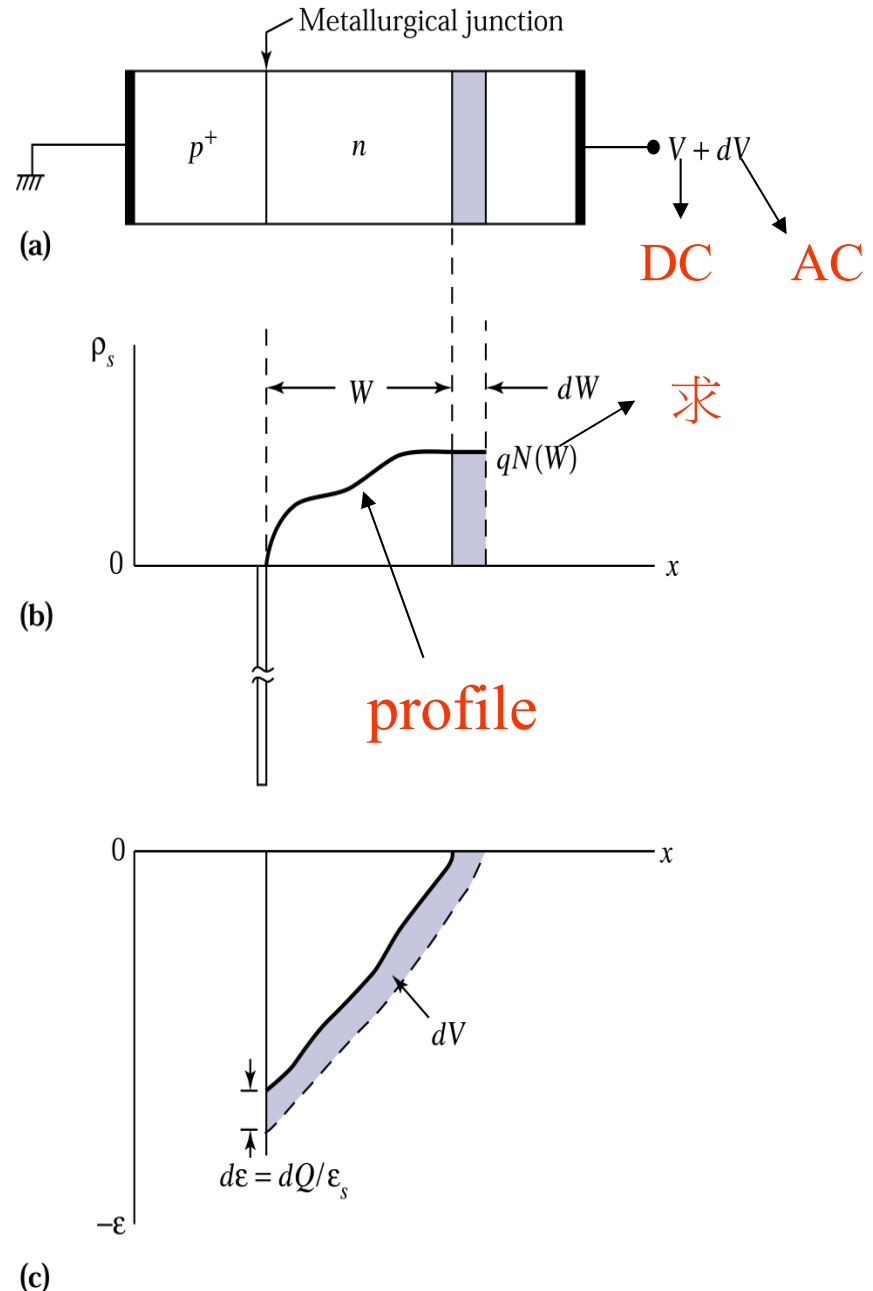
△ 測量 **doping profile** 用 C-V 法

## ○ abrupt junction

**Figure 3.12.**

(a)  $p^+$ - $n$  junction with an arbitrary impurity distribution. (b) Change in space charge distribution in the lightly doped side due to a change in applied bias. (c) Corresponding change in the electric-field distribution.

$$N(W) = \frac{2}{q\epsilon_s} \left( \frac{1}{d(1/C_j^2)} \right) \frac{dV}{dV}$$





**C<sub>j</sub> 正比 (V<sub>R</sub>)<sup>-n</sup>**

**n= ½ for abrupt**

**n=1/3 for linearly graded**

**C<sub>j</sub> 正比 (V<sub>R</sub>)<sup>-1/(m+2)</sup>**

**for hyperabrupt,  
Epitaxial growth**

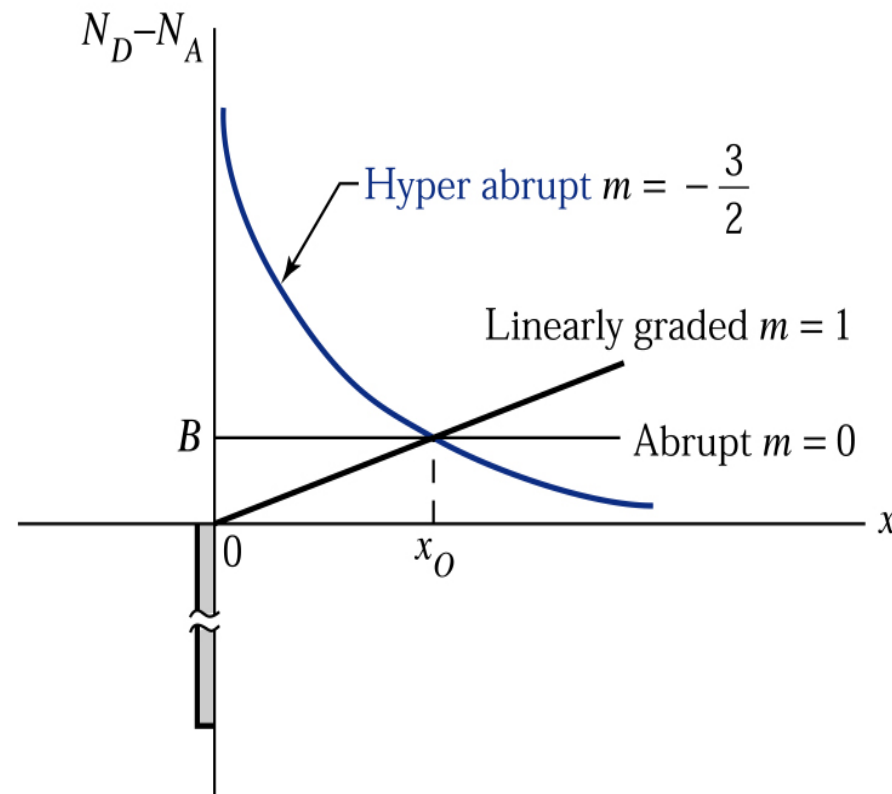
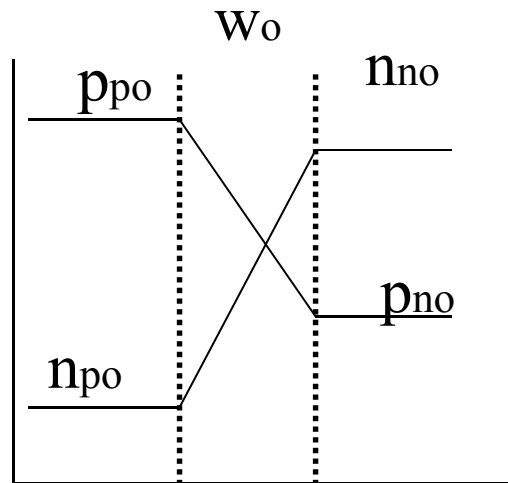


**Figure 3.13.** Impurity profiles for hyperabrupt, one-sided abrupt, and one-sided linearly graded junctions.

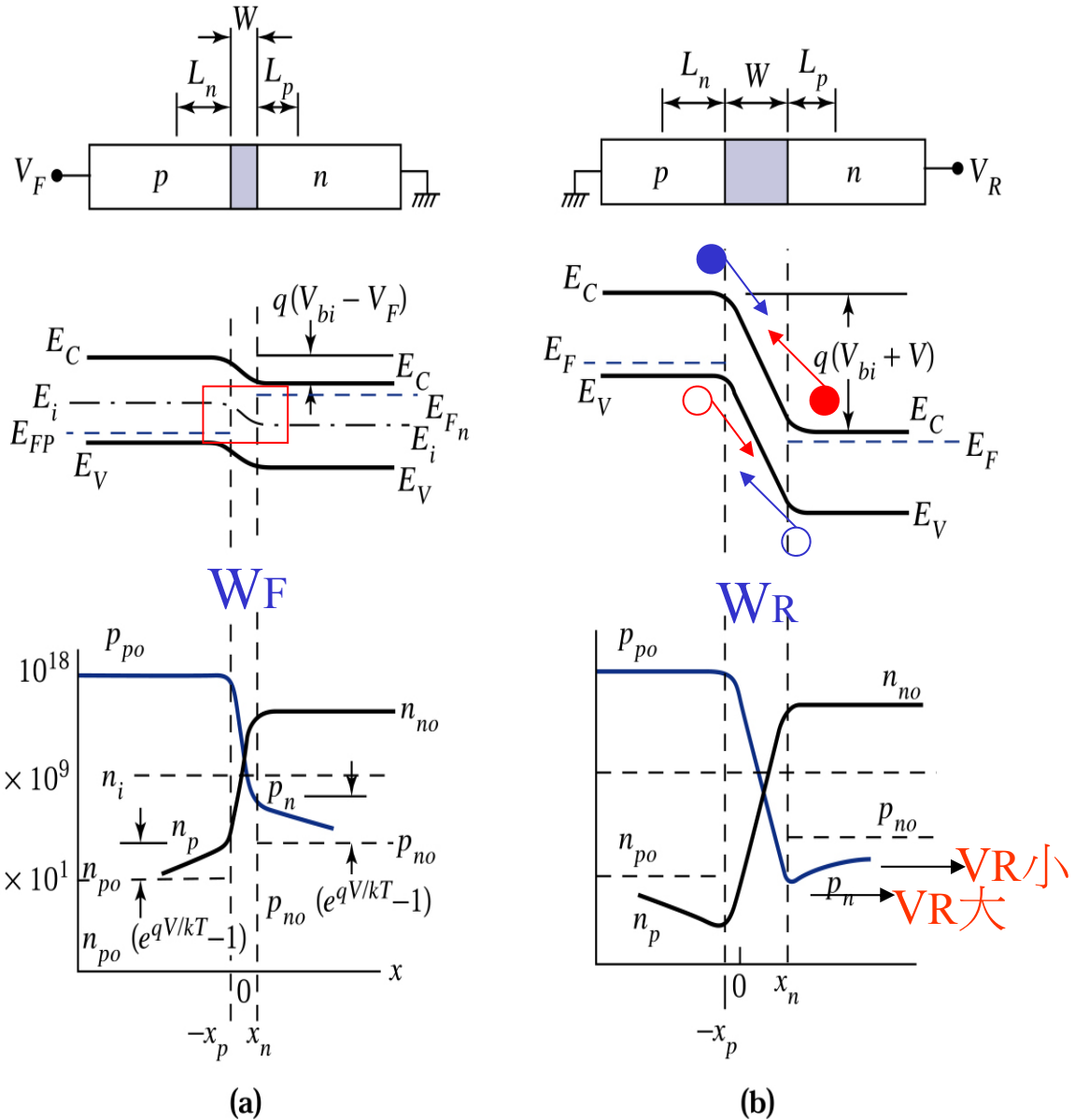
**Figure 3.14.**

Depletion region, energy band diagram and carrier distribution.

- (a) Forward bias.
- (b) Reverse bias.



Thermal equilibrium



Excess carrier

$$n_p - n_{po} = n_{po} \left( e^{qV/kT} - 1 \right).$$

$$p_n - p_{no} = p_{no} \left( e^{qV/kT} - 1 \right)$$

$$\therefore n_{no} = n_{po} e^{\frac{qV_{bi}}{kT}}$$

$$n_n = n_p e^{\frac{q(V_{bi} - V)}{kT}}, \quad \text{n}_n \sim \text{n}_{no}$$

$$n_p = n_{po} e^{\frac{qV}{kT}}$$

## Excess carrier

$$J_p(x_n) = -qD_p \frac{dp_n}{dx} \Big|_{x_n} = \frac{qD_p p_{no}}{L_p} \left( e^{qV/kT} - 1 \right).$$

$$J_n(-x_p) = qD_n \frac{dn_p}{dx} \Big|_{-x_p} = \frac{qD_n n_{po}}{L_n} \left( e^{qV/kT} - 1 \right)$$

$$\therefore \frac{d^2 p_n}{dx^2} - \frac{p_n - p_{no}}{D_p \tau_p} = 0$$

$$p_n = p_{no} + p_{no} \left( e^{\frac{qV}{kT}} - 1 \right) e^{\frac{-(x-x_n)}{L_p}}$$

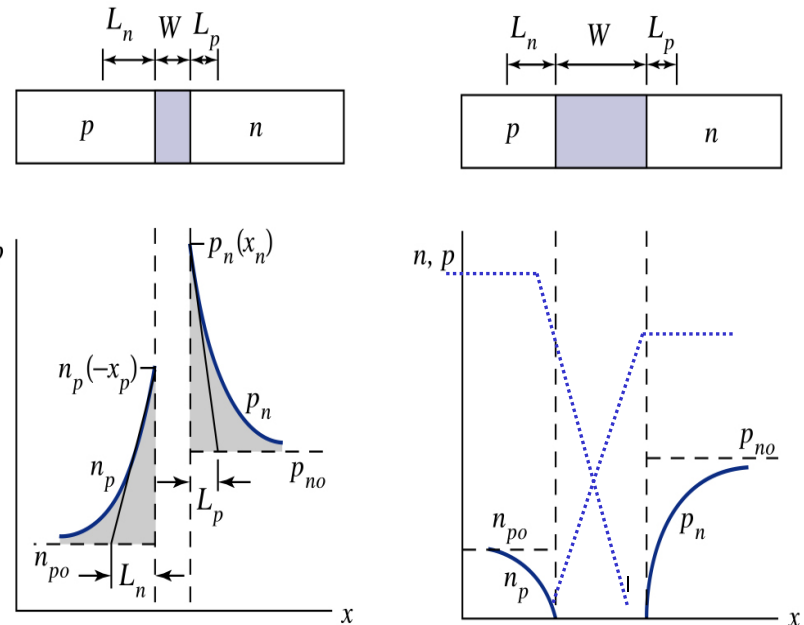
**Figure 3.15.**

Injected minority carrier distribution and electron and hole currents. (a) Forward bias. (b) Reverse bias. The figure illustrates idealized currents. For practical devices, the currents are not constant across the space charge layer.

$$p^+ / n$$

$\downarrow$

$J_p \gg J_n$



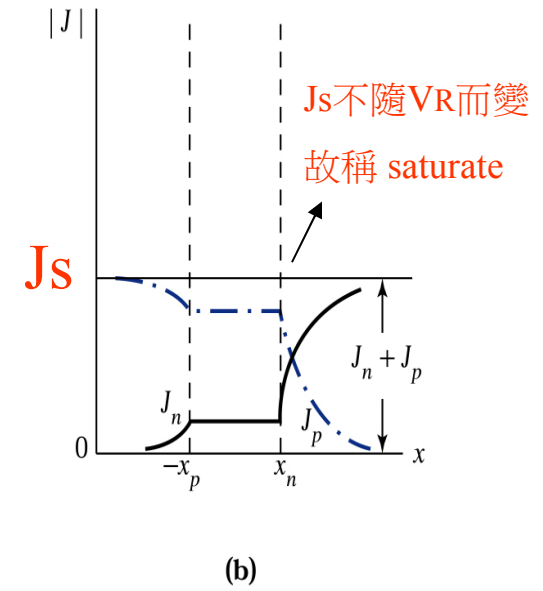
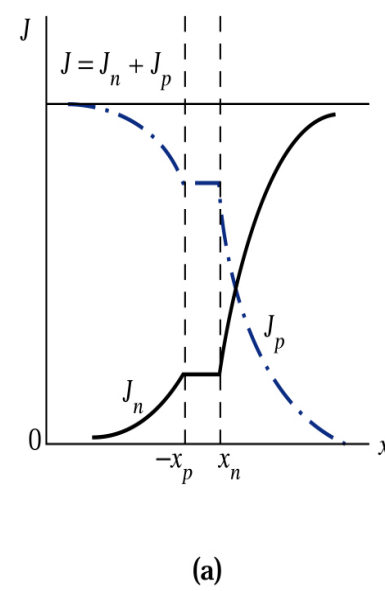
Ideal diode eq.(僅求diff. current)

$$J = J_p(x_n) + J_n(-x_p) = J_s \left( e^{qV/kT} - 1 \right),$$

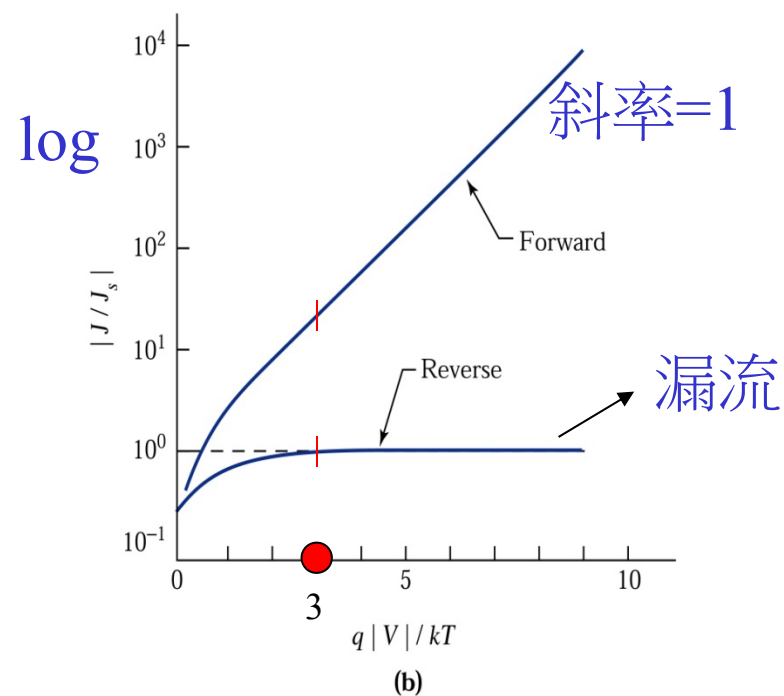
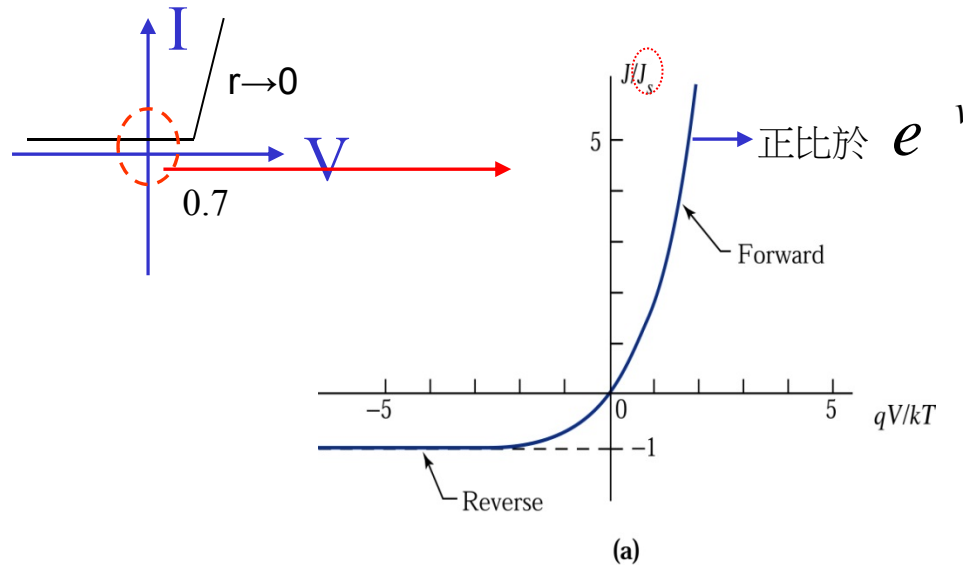
V為負時,可略 .J=Js為定值

$$J_s \equiv \frac{qD_p p_{no}}{L_p} + \frac{qD_n n_{po}}{L_n},$$

:sat. current density



**Figure 3.16.**  
**Ideal** current-voltage  
 characteristics.  
 (a) Cartesian plot.  
 (b) Semilog plot.



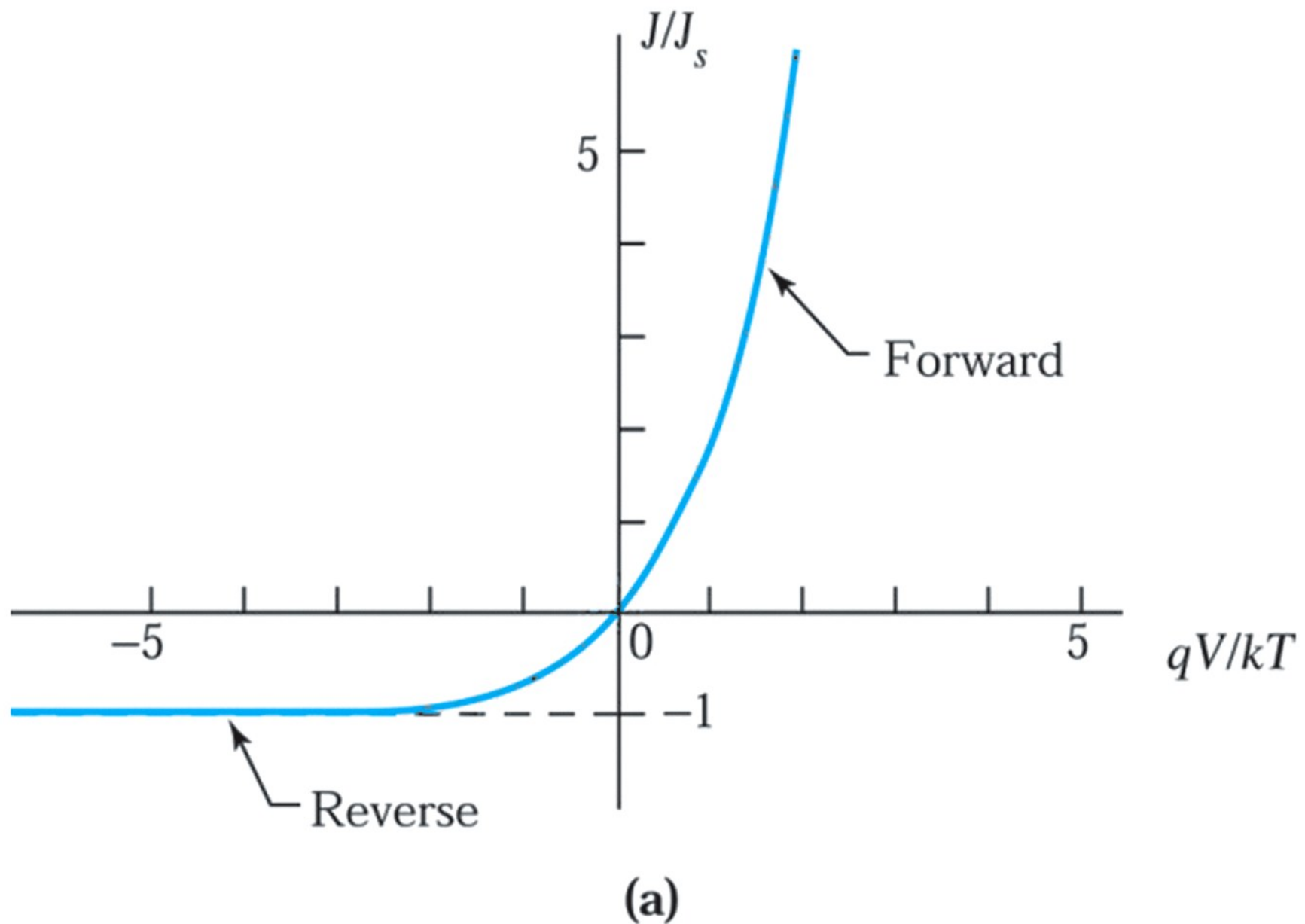


Figure 3.16a  
© John Wiley & Sons, Inc. All rights reserved.

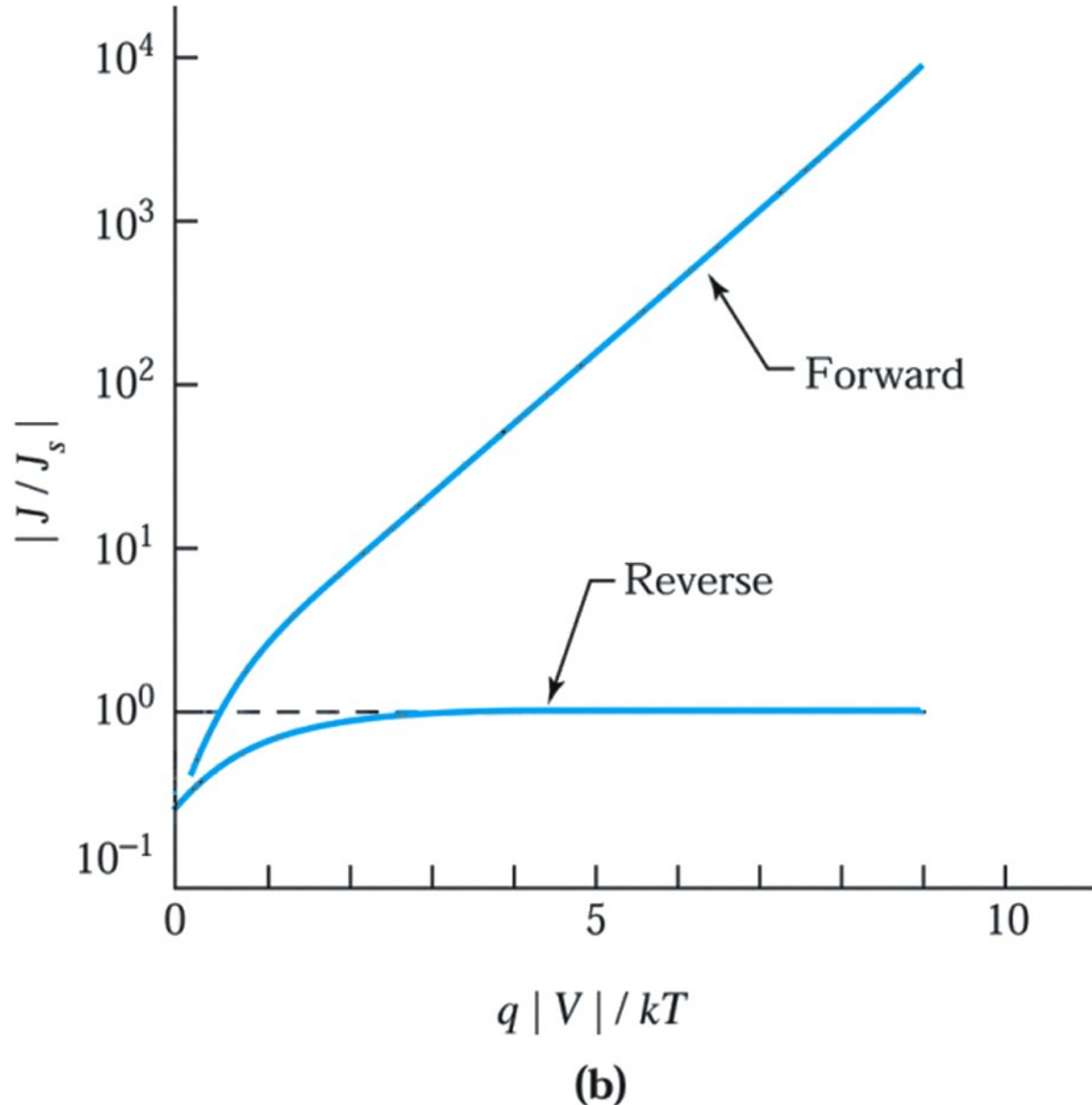


Figure 3.16b  
© John Wiley & Sons, Inc. All rights reserved.

## Generation-Recombination and high-injection Effect\*

$$G = -U \approx \left[ \frac{\sigma_p \sigma_n V_{th} N_t}{\sigma_n \exp\left[\frac{E_t - E_i}{kT}\right] + \sigma_p \exp\left[\frac{E_i - E_t}{kT}\right]} \right] = \frac{n_i}{\tau_g}$$

空乏區之產生電流

(因為  $G \equiv n_i / \tau_g$ )

Assume  $\sigma_n = \sigma_p = \sigma_0$

$$G \approx \frac{\sigma_0 V_{th} N_t n_i}{2 \cosh\left[\frac{E_t - E_i}{kT}\right]}$$

$G = \text{Max}$  at  $E_t = E_i$

## Generation-Recombination and high-injection Effect\*

空乏區之產生電流

(因為  $G \equiv n_i / \tau_g$ )

$$J_{gen} = \int_0^W qGdx \cong qGW = \frac{qn_i W}{\tau_g}$$

For p+/n ( $N_A \gg N_D$ ) (55a)

( $J_{diff}$  為  $VR \geq 3kT/q$   
下由(55)得到)

反向  $J_R \cong q \sqrt{\frac{D_p}{\tau_p}} \frac{n_i^2}{N_D} + \frac{qn_i W}{\tau_g}.$

Ge:  $n_i$  大 ,  $J_{diff}$  dominate  
Si :  $n_i$  小 ,  $J_{gen}$  dominate

## Recombination Effect\*

$$n_n p_n \cong n_{n0} p_{n0} e^{qV/kT} = n_i^2 e^{qV/kT}$$

Assume  $\sigma_n = \sigma_p = \sigma_0$

$$U \approx \frac{\sigma_0 V_{th} N_t n_i^2 (e^{qV/kT} - 1)}{n_n + p_n + 2n_i \cosh \frac{E_i - E_t}{kT}}$$

at  $E_t = E_i$

$$U \approx \sigma_0 V_{th} N_t \frac{n_i^2 (e^{qV/kT} - 1)}{n_n + p_n + 2n_i}$$

## Recombination Effect\*

At  $n_n + p_n = \text{min.}$ ,  $U = \text{Max.}$

$$n_n p_n = \text{常數}$$

$$dn_n p_n + n_n dp_n = 0$$

$$-dn_n = \frac{n_n}{p_n} dp_n$$

$$d(p_n + n_n) = 0$$

$$dp_n = -dn_n = \frac{n_n}{p_n} dp_n$$

$$p_n = n_n = n_i e^{qV/2kT}$$

$$U_{\max} \approx \sigma_0 V_{th} N_t \frac{n_i^2 (e^{qV/kT} - 1)}{2n_i (e^{qV/2kT} + 1)}$$

$$U_{\max} \approx \frac{1}{2} \sigma_0 V_{th} N_t n_i e^{qV/2kT}$$

## Recombination Effect\*

$$J_{rec} = \int_0^W qUdx \approx \frac{qW}{2} \sigma_o v_{th} N_t n_i e^{qV/2kT} = \frac{qWn_i}{2\tau_r} e^{qV/2kT}$$

$$J_F = q \sqrt{\frac{D_p}{\tau_p}} \frac{n_i^2}{N_D} e^{qV/kT} + \frac{qWn_i}{2\tau_r} e^{qV/2kT}$$

$$J_F \approx \exp\left(\frac{qV}{\eta kT}\right), \quad 1 < \eta < 2$$

Where the factor  $\eta$  is called the ideality factor

p / n junction 好壞之重要參數

串聯電阻和 high level inj.

**Figure 3.17.**

Comparison of the forward current-voltage characteristics of Si and GaAs diodes<sup>2</sup> at 300 K. Dashed lines indicate slopes of different ideality factors  $\eta$ .

ref:(69)

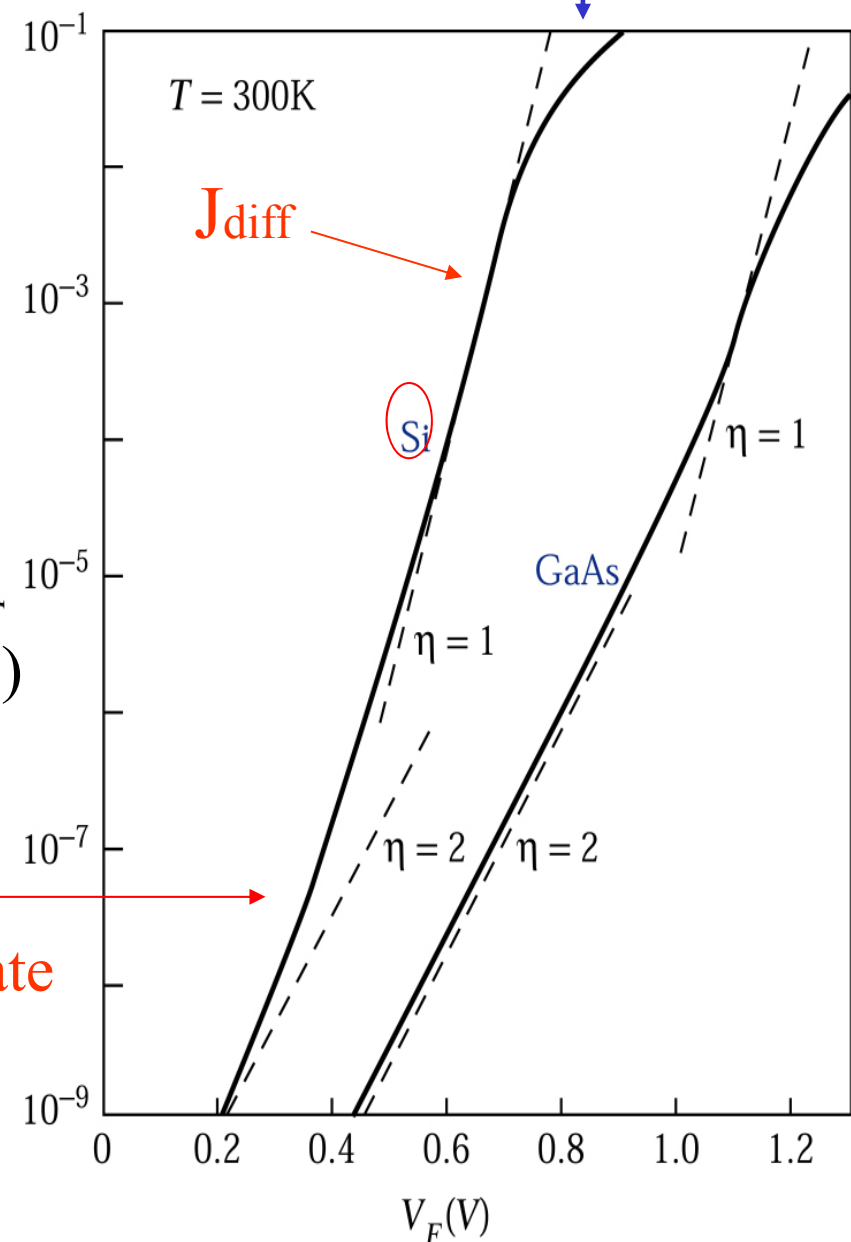
\*high level injection:( p+-n 為例)

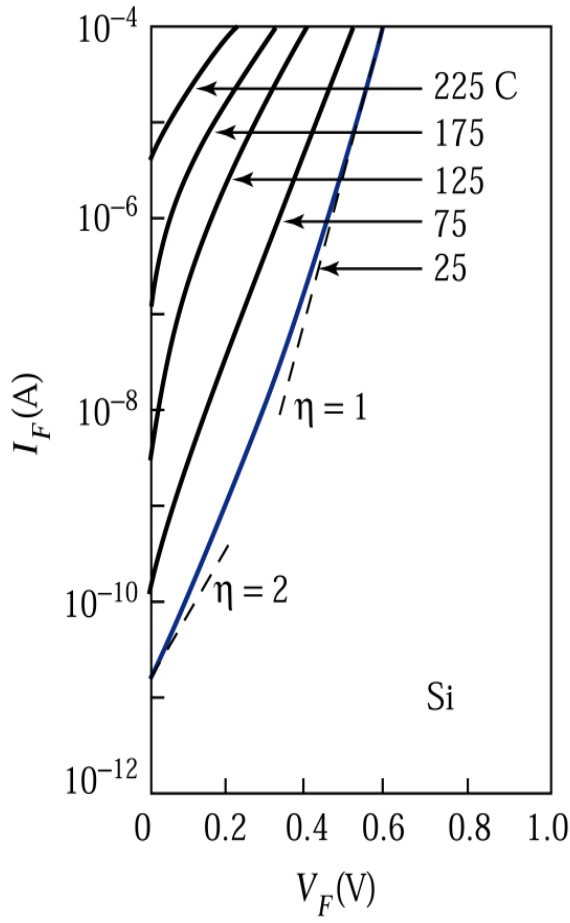
$$\text{即 } p_n(x_n) \approx n_{no}$$

$$\text{由(60) } p_n n_n = n_i^2 e^{\frac{qV}{kT}} \quad J_{rec}$$

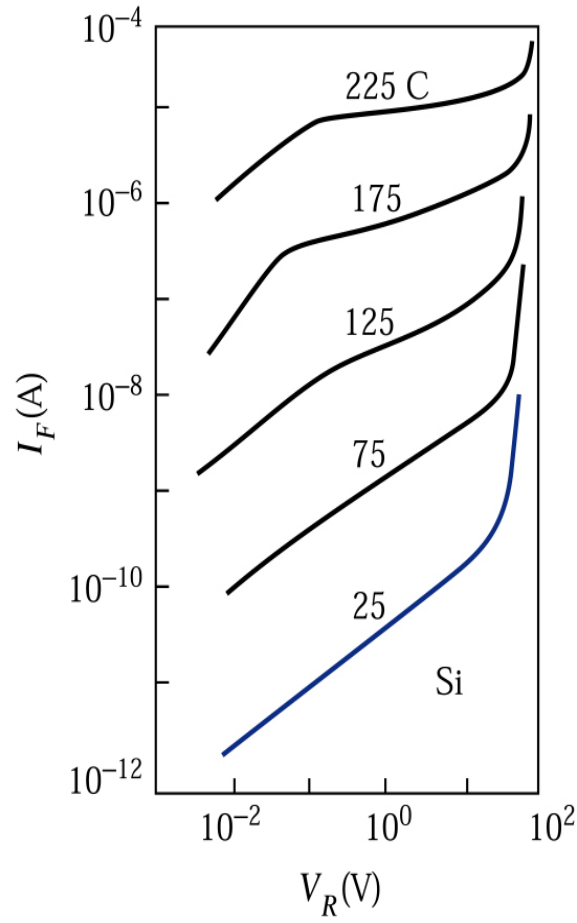
$$\text{故 } p_n \approx n_n \approx n_i e^{\frac{qV}{2kT}} \quad \text{dominate}$$

電流增加較緩





(a)



(b)

- (a) With increasing temp, increase of  $I_{diff} > I_{recom}$  due to  $J_s$
  - (b) Low temp,  $J_g$  dominate  $\sim (V_R)^{1/2}$ ; high temp,  $J_s$  dominate
- Trap analysis should be low temp**

**Figure 3.18.** Temperature dependence of the current-voltage characteristics of a Si diode<sup>2</sup>. (a) Forward bias. (b) Reverse bias.

## Minority Carrier Storage

☆在Forward bias 會有

excess

$$Q_p = q \int_{x_n}^{\infty} (p_n - p_{no}) dx,$$

$$= q \int_{x_n}^{\infty} p_{no} \left( e^{qV/kT} - 1 \right) e^{-(x-x_n)/L_p} dx,$$

$$= q L_p p_{no} \left( e^{qV/kT} - 1 \right).$$

$$Q_p = \frac{L_p^2}{D_p} J_p(x_n) = \tau_p J_p(x_n).$$

Minority life time

電流

# Diffusion Capacitance

☆在 forward bias 下：

\*反向有  $C_j$

\*順向有  $C_d$

definition  $C_d = A dQ_p / dV$  dV 指 A.C.

$$C_d = \frac{Aq^2 L_p p_{no}}{kT} e^{qV/kT}$$

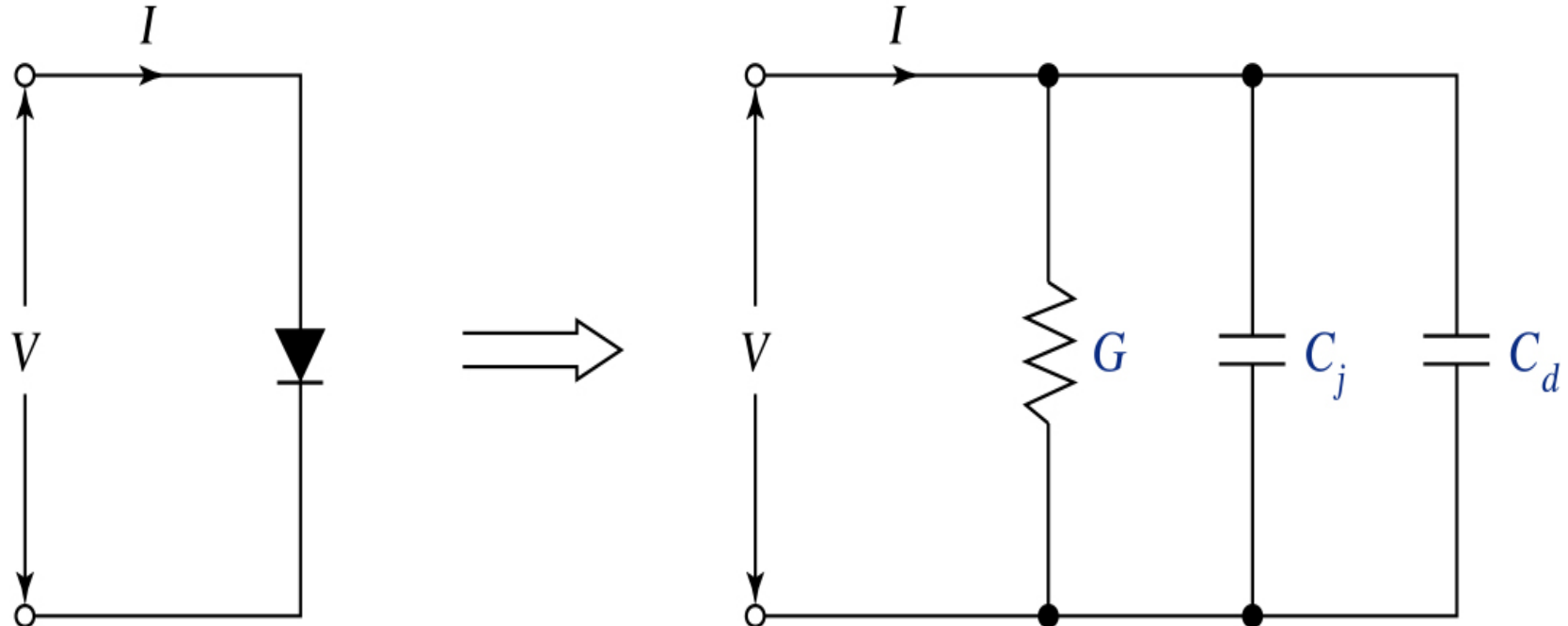


**Figure 3.19.** Small-signal equivalent circuit of a *p-n* junction.

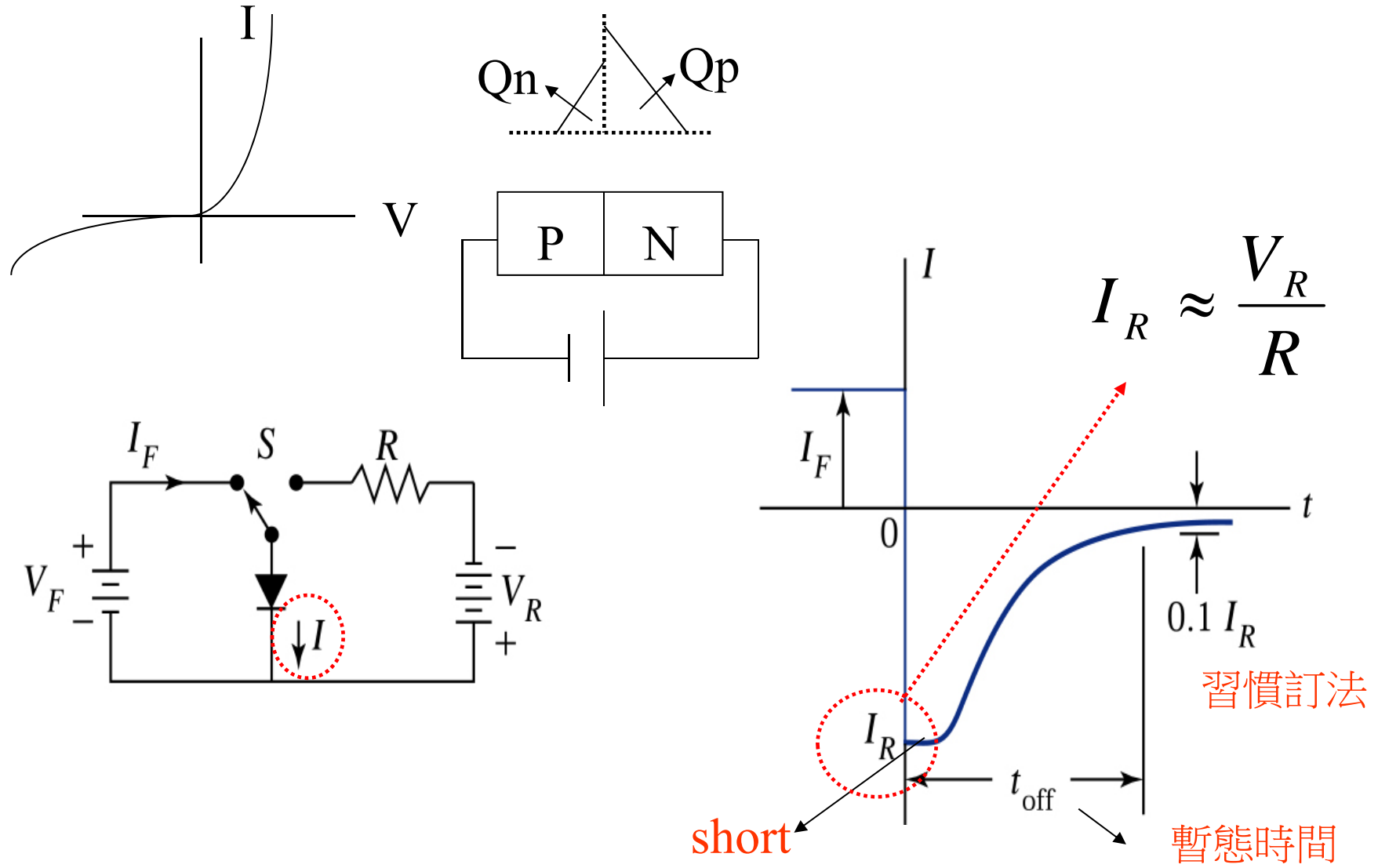


**Figure 3.20.** Transient behavior of a  $p-n$  junction (a) Basic switching circuit. (b) Transient response of the current switched from forward bias to reverse bias.

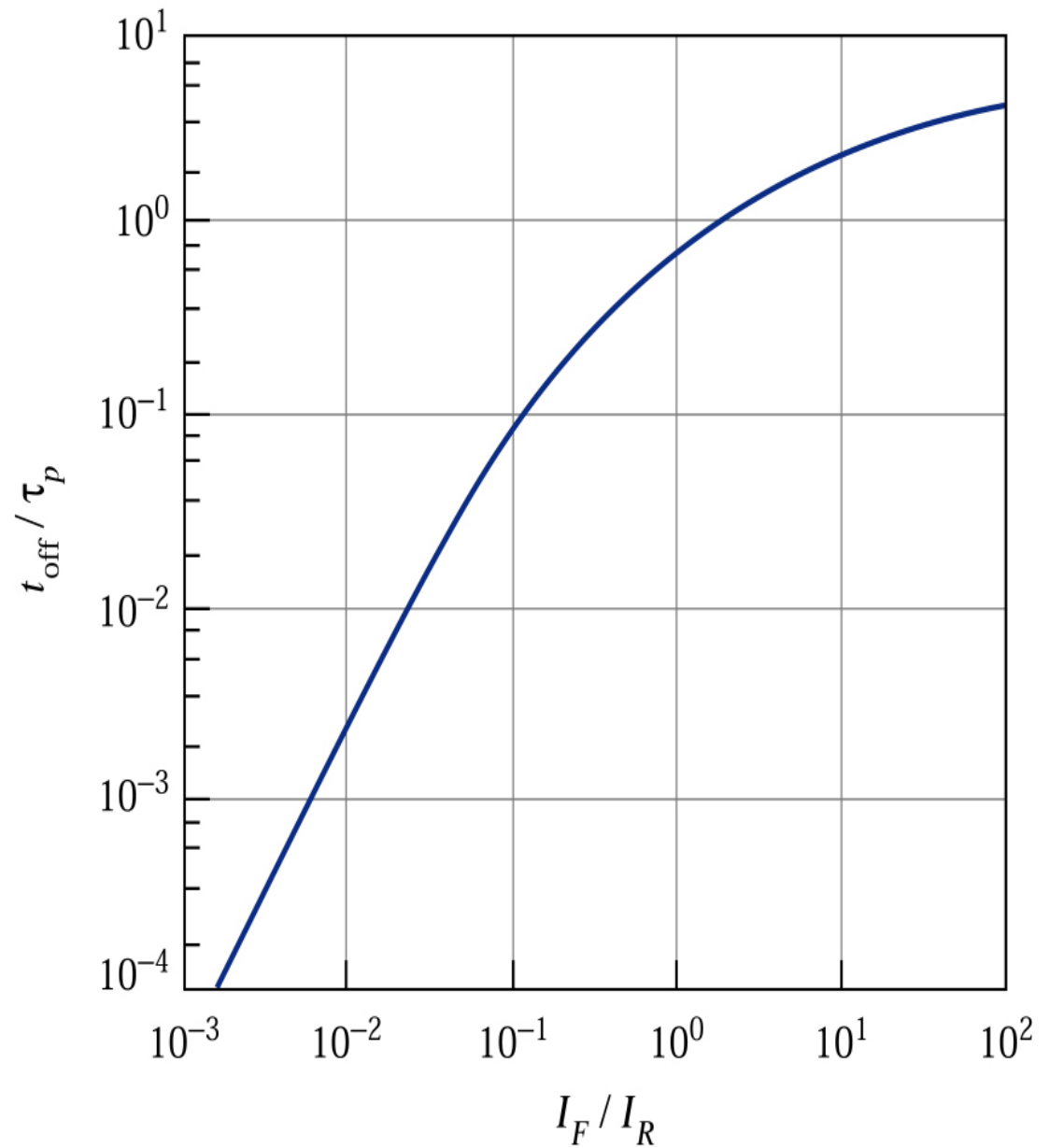
- $t_{off} \downarrow$  越好

$$t_{off} \approx \frac{Q_p A}{I_{R,ave}} = \tau_p \left[ \frac{I_F}{I_{R,ave}} \right]$$

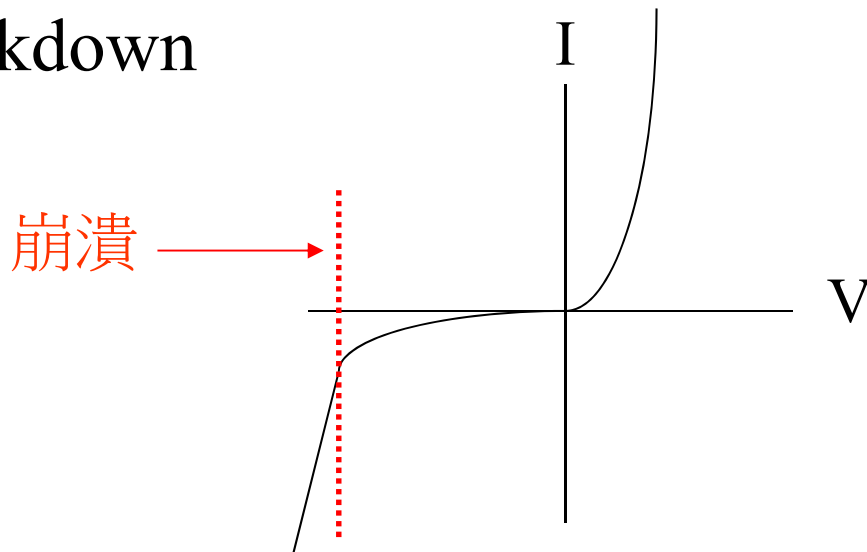
☆ For 快速switch，使  $\tau_{p\downarrow}$

⇒ 在  $E_i$  增加 G-R center  
(doping **Au** 等)

**Figure 3.21.**  
Normalized transient time  
versus the ratio of forward  
current to reverse current.<sup>3</sup>



\*Junction breakdown



\*Tunneling Effect

☆ p , n 濃度都很高(W小)

\*Avalanche Multiplication

impact ionization

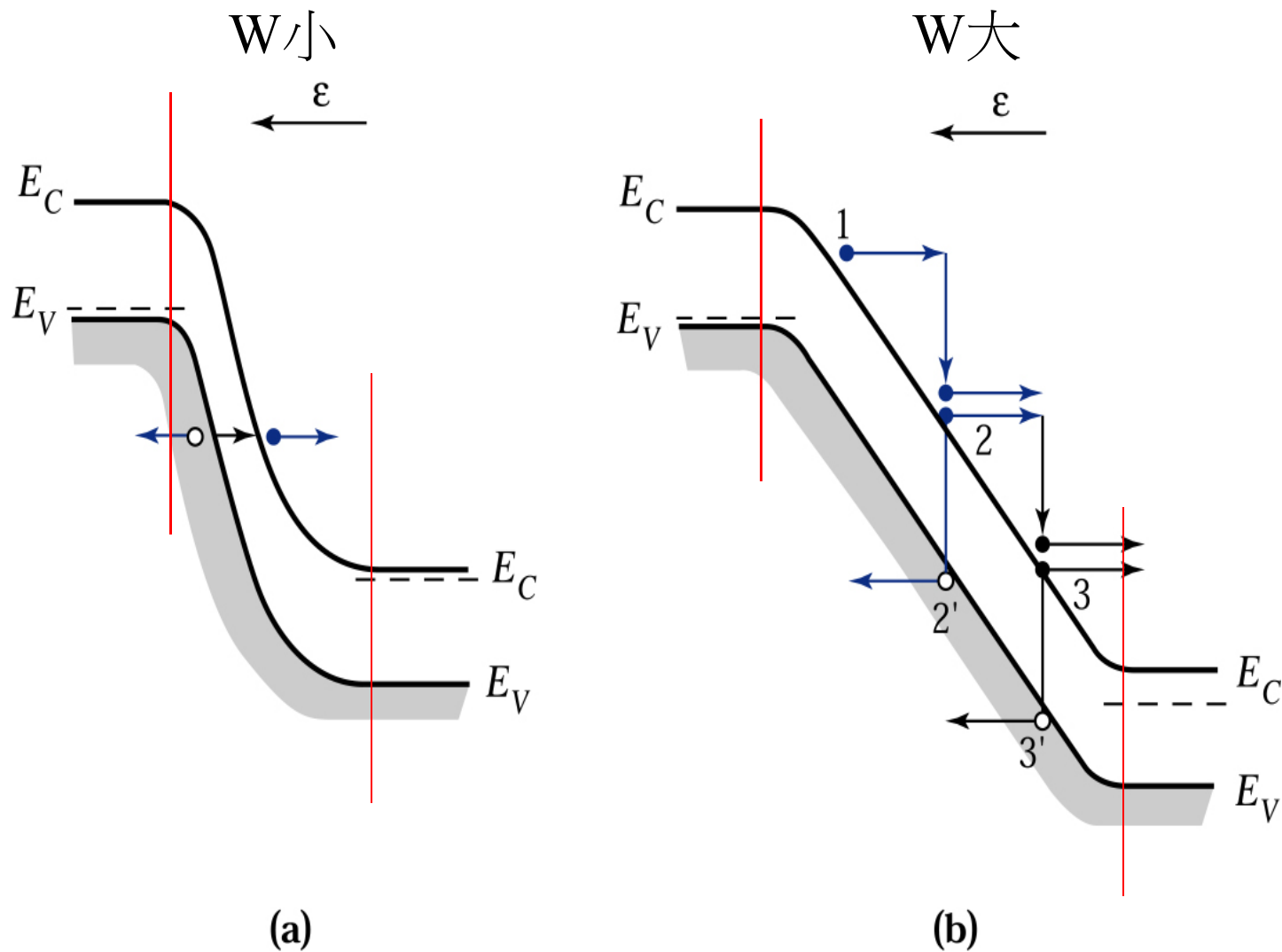


**Figure 3.22.** Energy band diagrams under junction-breakdown conditions.  
 (a) Tunneling effect (b) Avalanche multiplication.

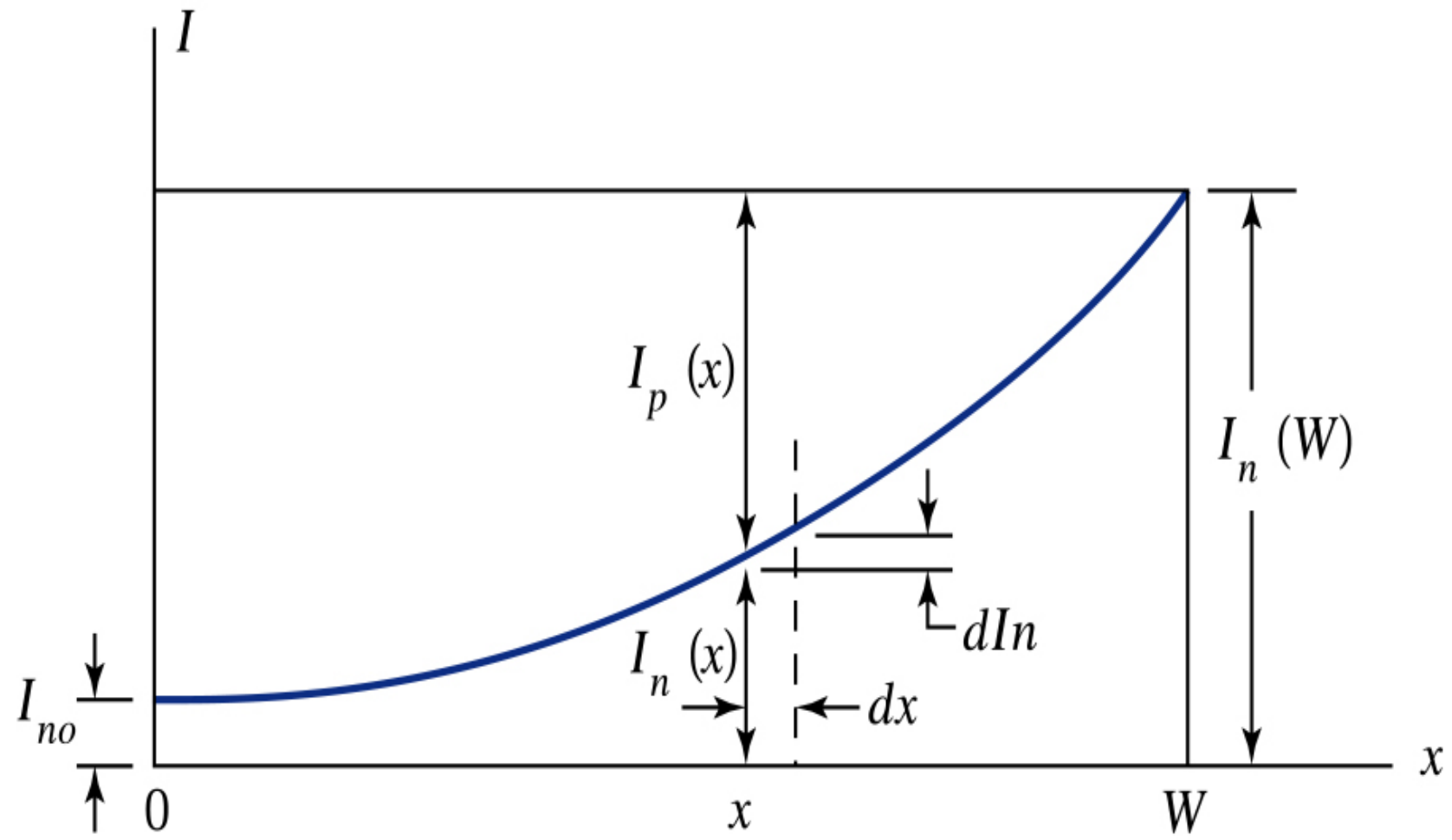


**Figure 3.23.** Depletion region in a  $p$ - $n$  junction with multiplication of an incident current.

$$V_B \text{ (breakdown voltage)} = \frac{E_c W}{2} = \frac{\epsilon_s E_c^2}{2q} (N_B)^{-1}$$

$\mathbf{NB} \uparrow \rightarrow \mathbf{V}_B \downarrow$

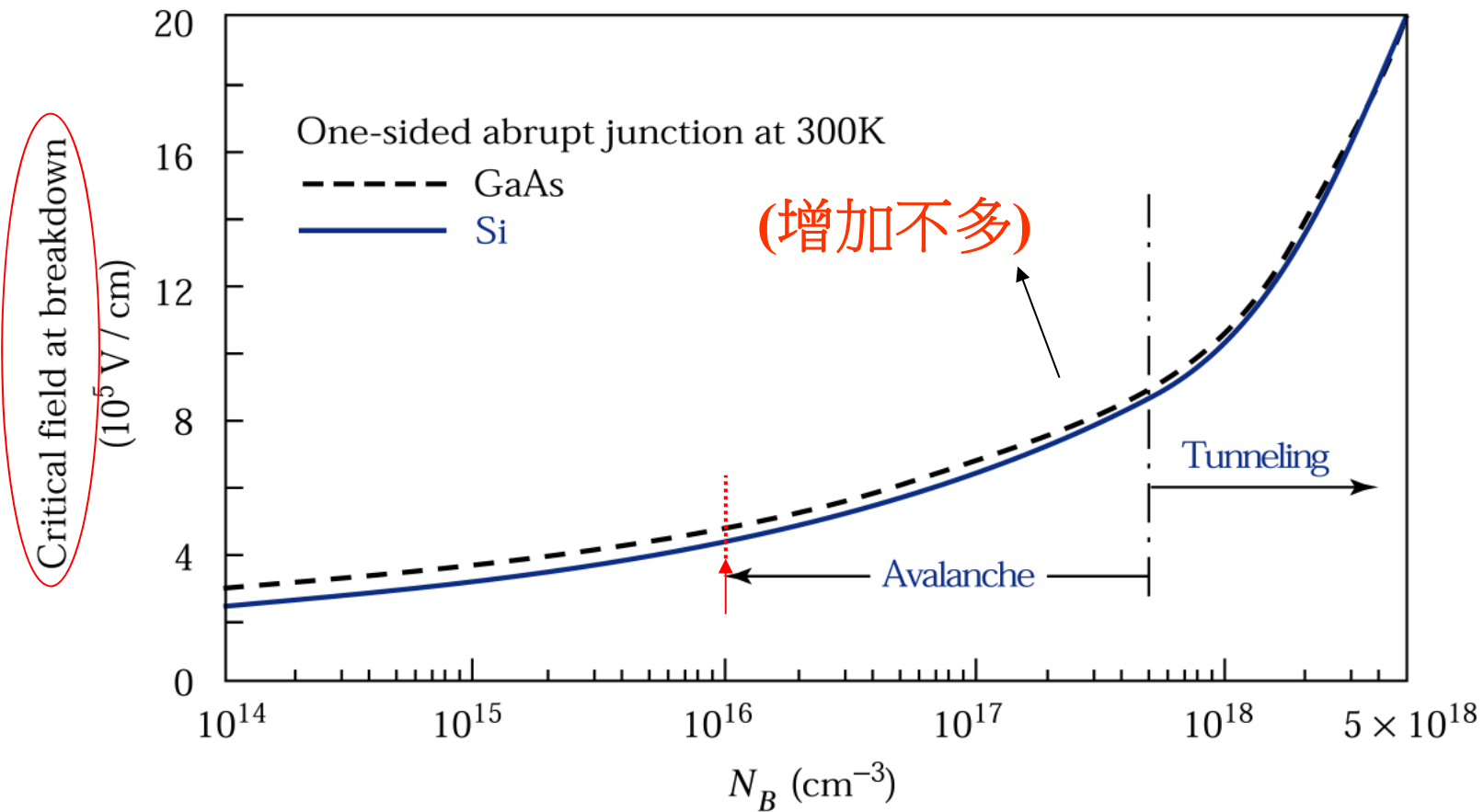


**Figure 3.24.** Critical field at breakdown versus background doping for Si and GaAs one-sided abrupt junctions.<sup>5</sup>

**Figure 3.25.**  
 Avalanche breakdown voltage versus impurity concentration for one-sided abrupt junction and avalanche breakdown voltage versus impurity gradient for linearly graded junction in Si and GaAs. **Dash-dot line indicates the onset of the tunneling mechanism.<sup>5</sup>**

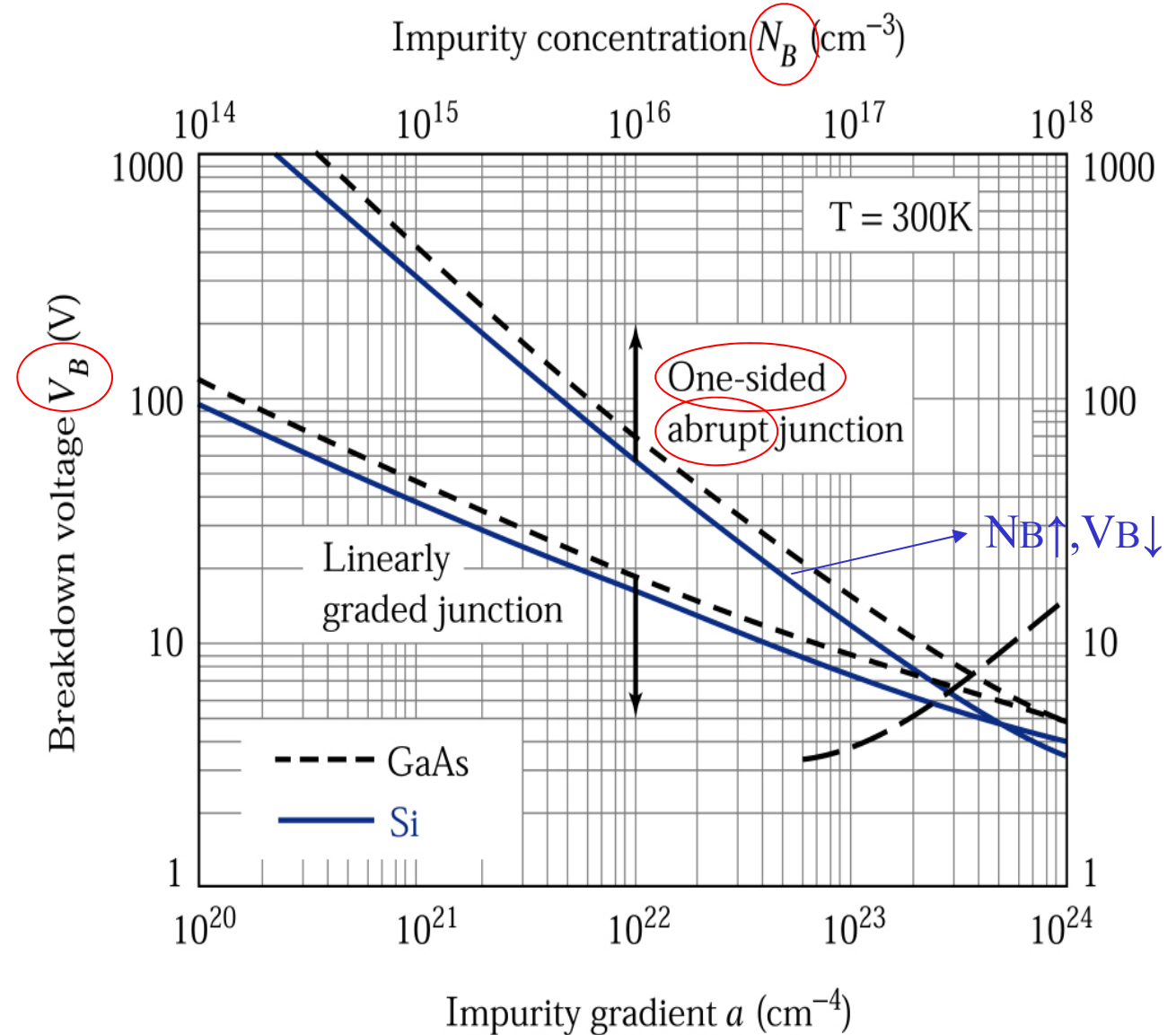
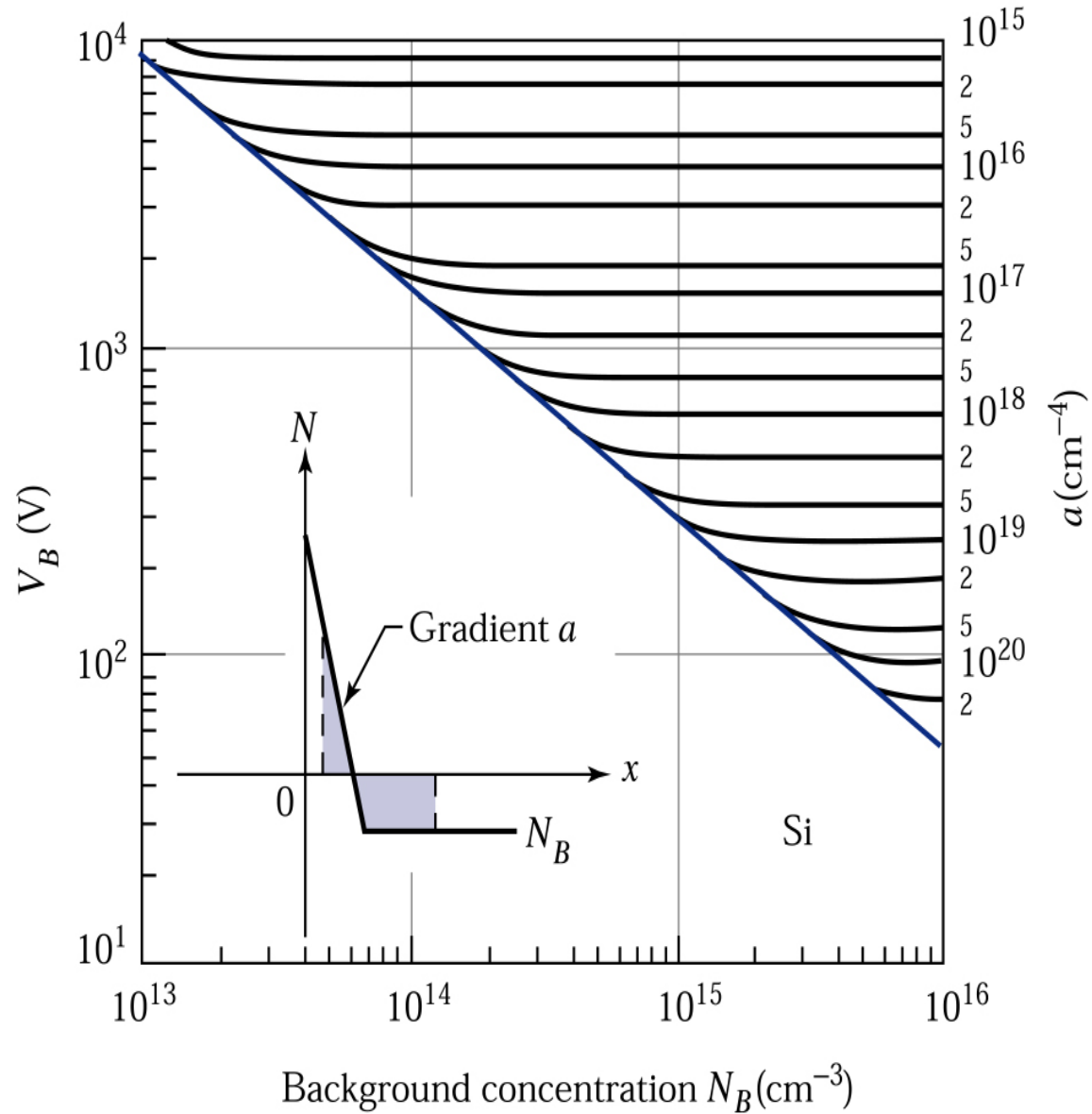


**Figure 3.26.**  
Breakdown voltage for  
diffused junctions.  
Inset shows the space  
charge distribution.<sup>6</sup>



**N<sub>B</sub> ↓, a ↓, V<sub>B</sub> ↑**

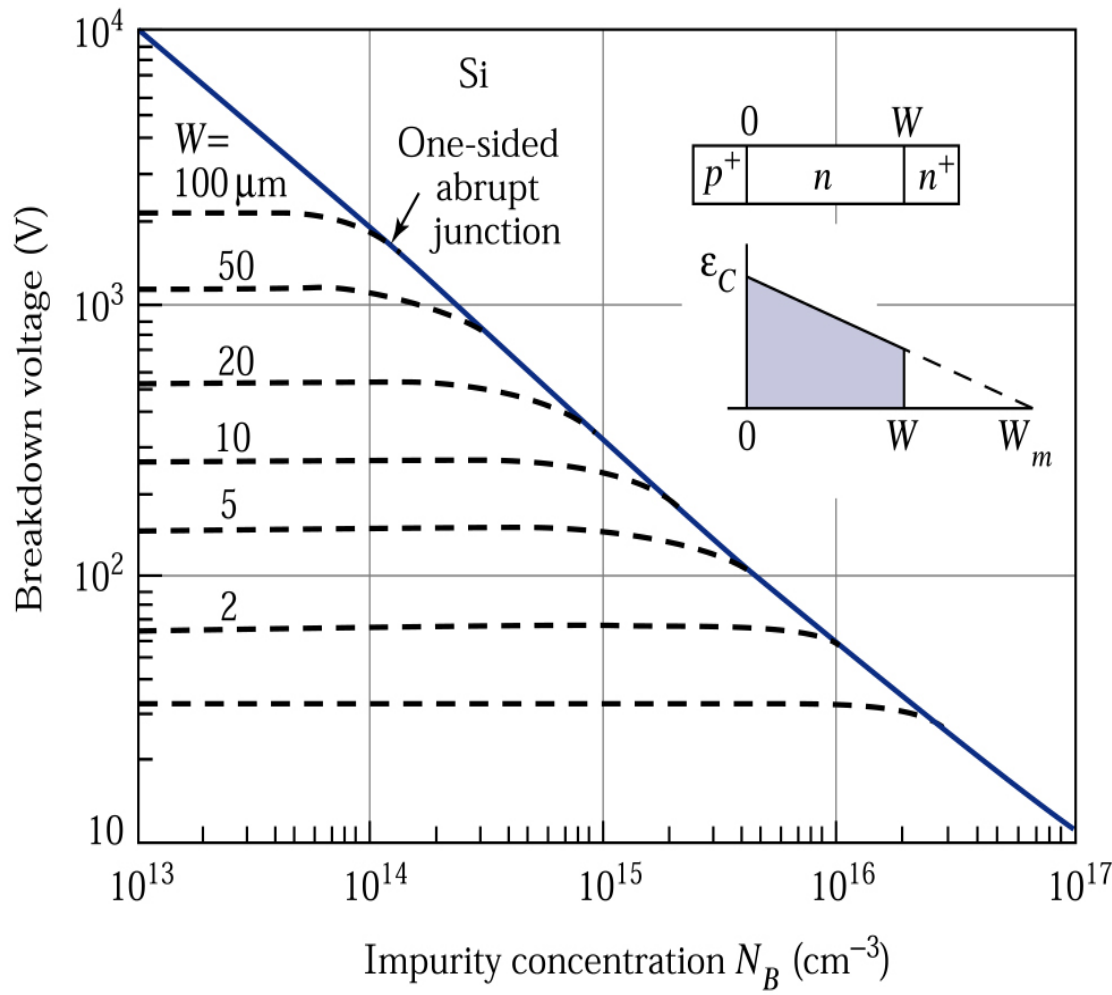
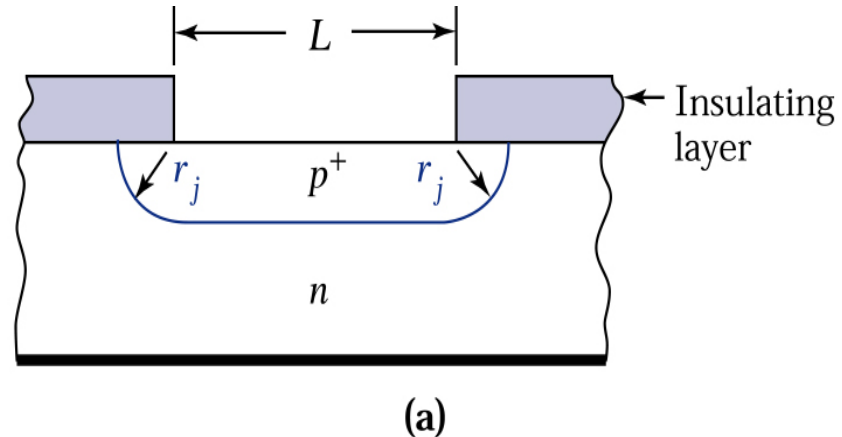


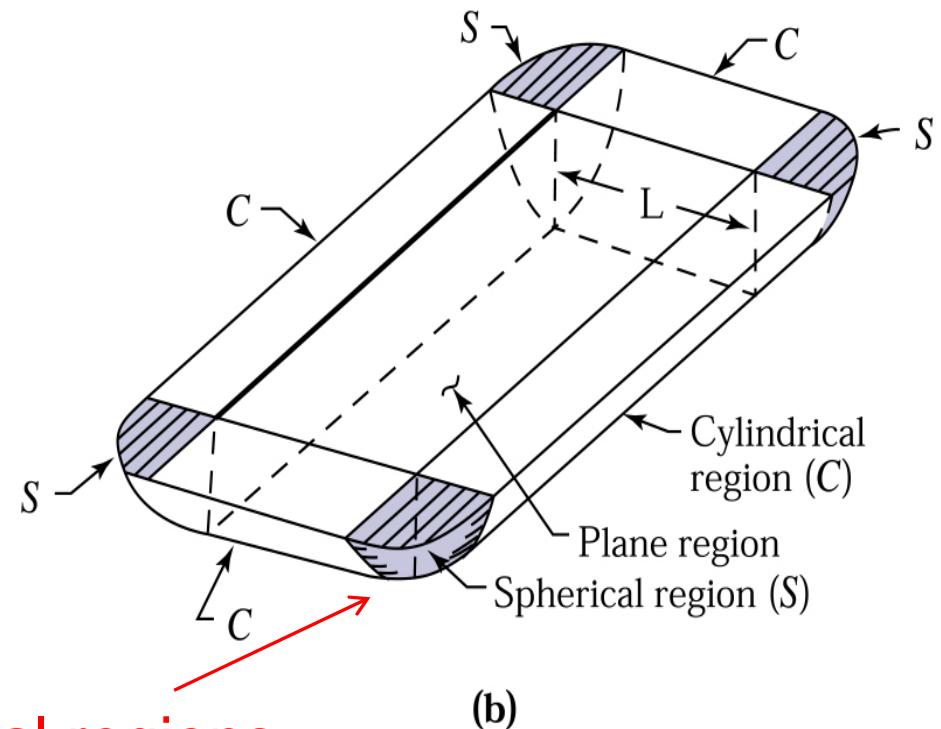
**Figure 3.27.** Breakdown voltage for  $p^+-\pi-n^+$  and  $p^+-v-n^+$  junctions.  $W$  is the thickness of the **lightly doped  $p$ -type ( $\pi$ ) or the lightly doped  $n$ -type ( $v$ ) region.**

**Figure 3.28.**

(a) Planar diffusion process that forms junction curvature near the edge of the diffusion mask, where  $r_j$  is the radius of curvature. (b) Cylindrical and spherical regions formed by diffusion through a rectangular mask.



(a)



(b)

Breakdown occurs in spherical regions

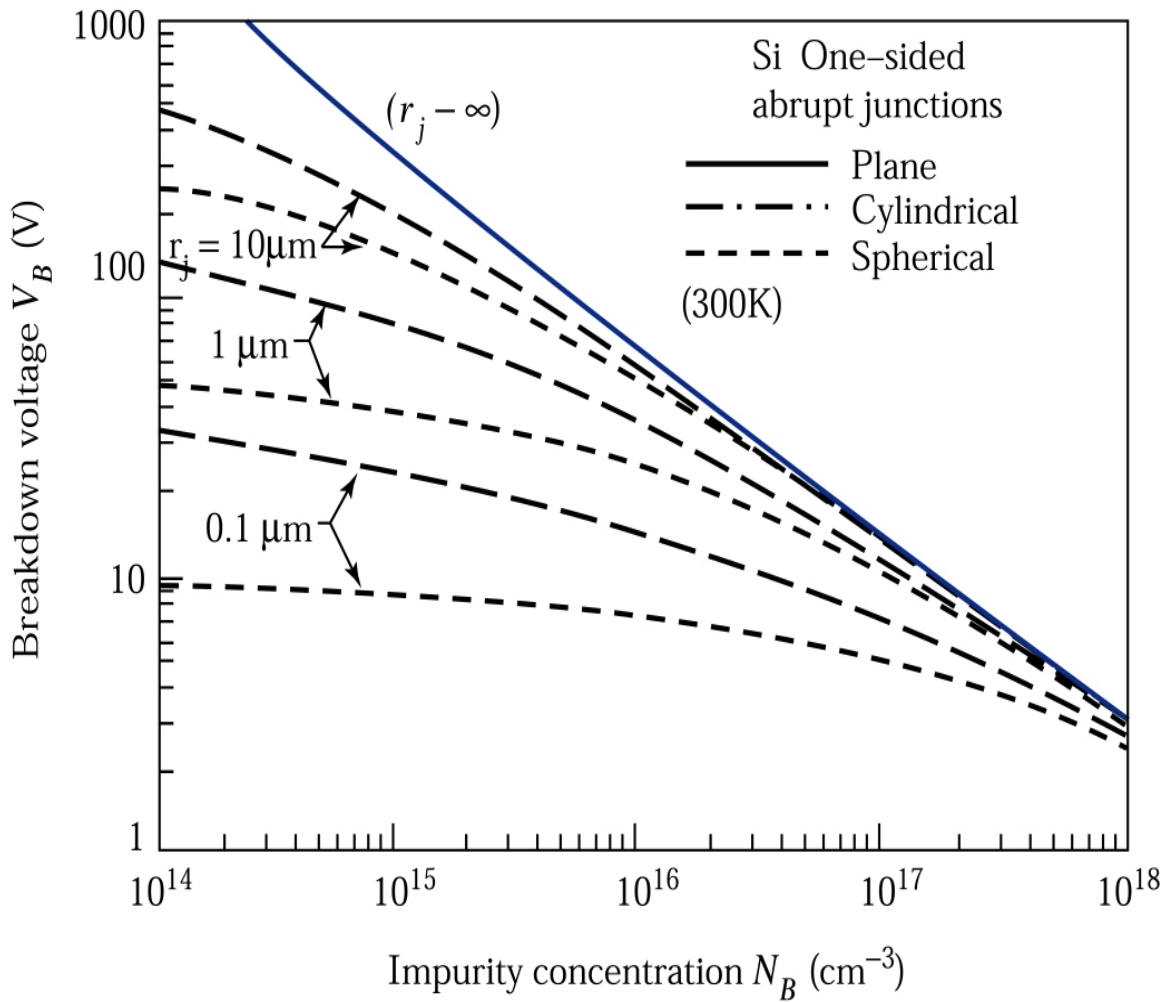
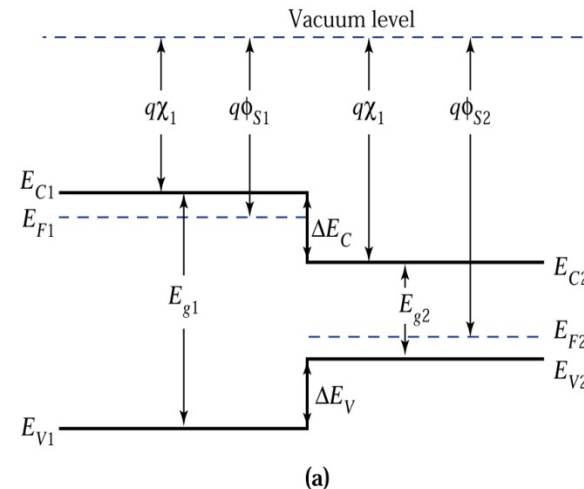


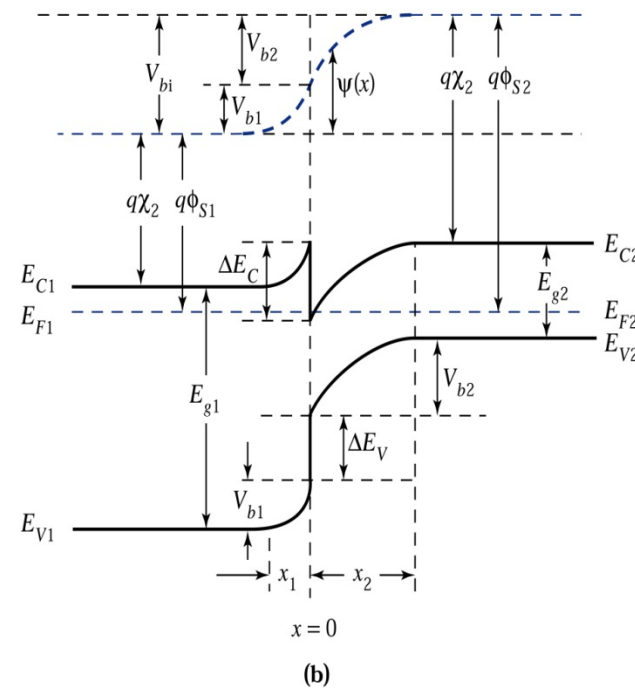
**Figure 3.29.** Breakdown voltage versus impurity concentration for one-sided abrupt doping profile with cylindrical and spherical junction geometries,<sup>7</sup> where  $r_j$  is the radius of curvature indicated in Fig. 3.28..

**Figure 3.30.**

- (a) Energy band diagram of two isolated semiconductors.  
 b) Energy band diagram of an ideal ***n-p*** heterojunction at thermal equilibrium.



(a)



(b)

Band offset:  $\Delta E_C$ ,  $\Delta E_V$   
 Band alignment

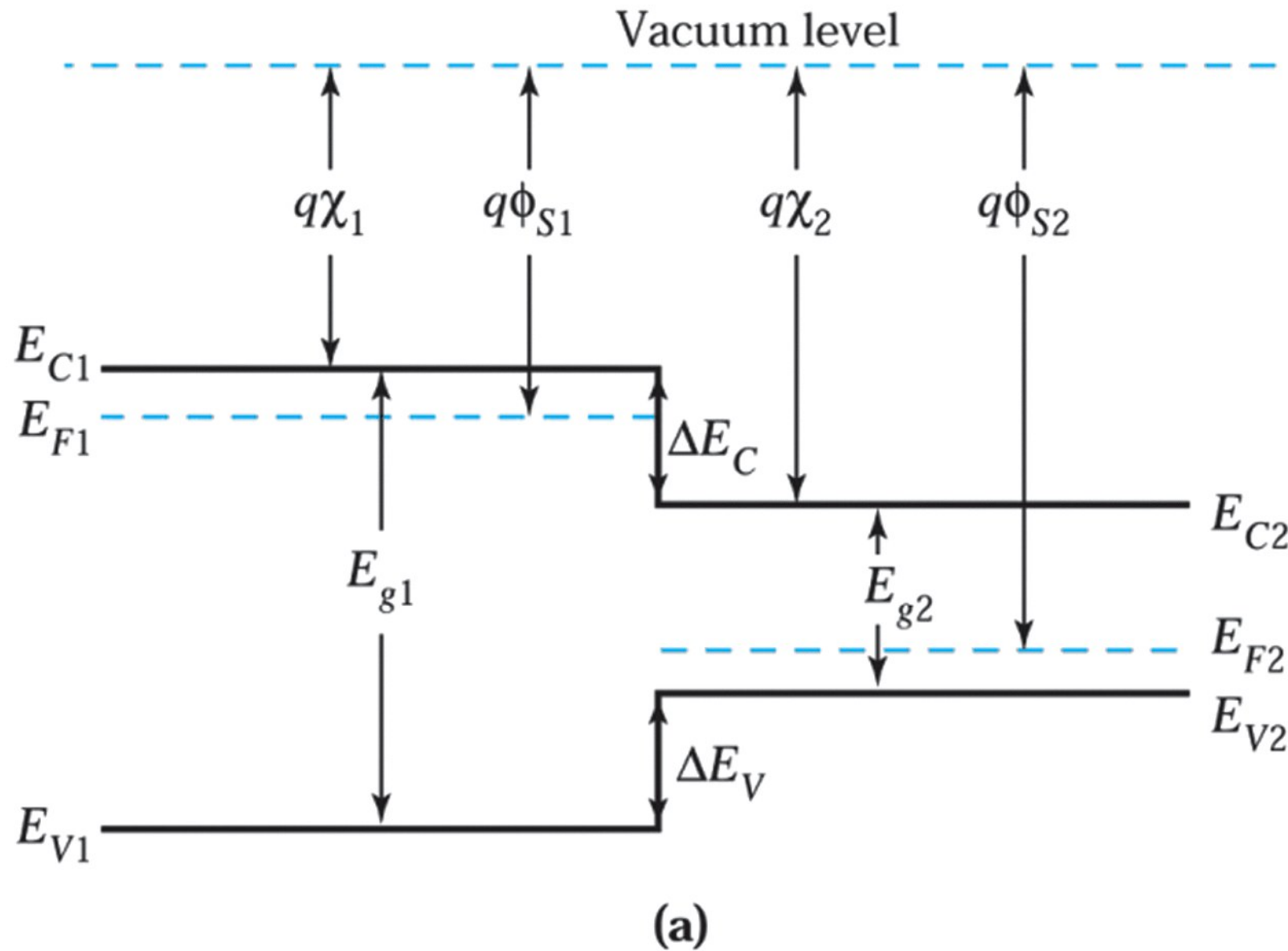
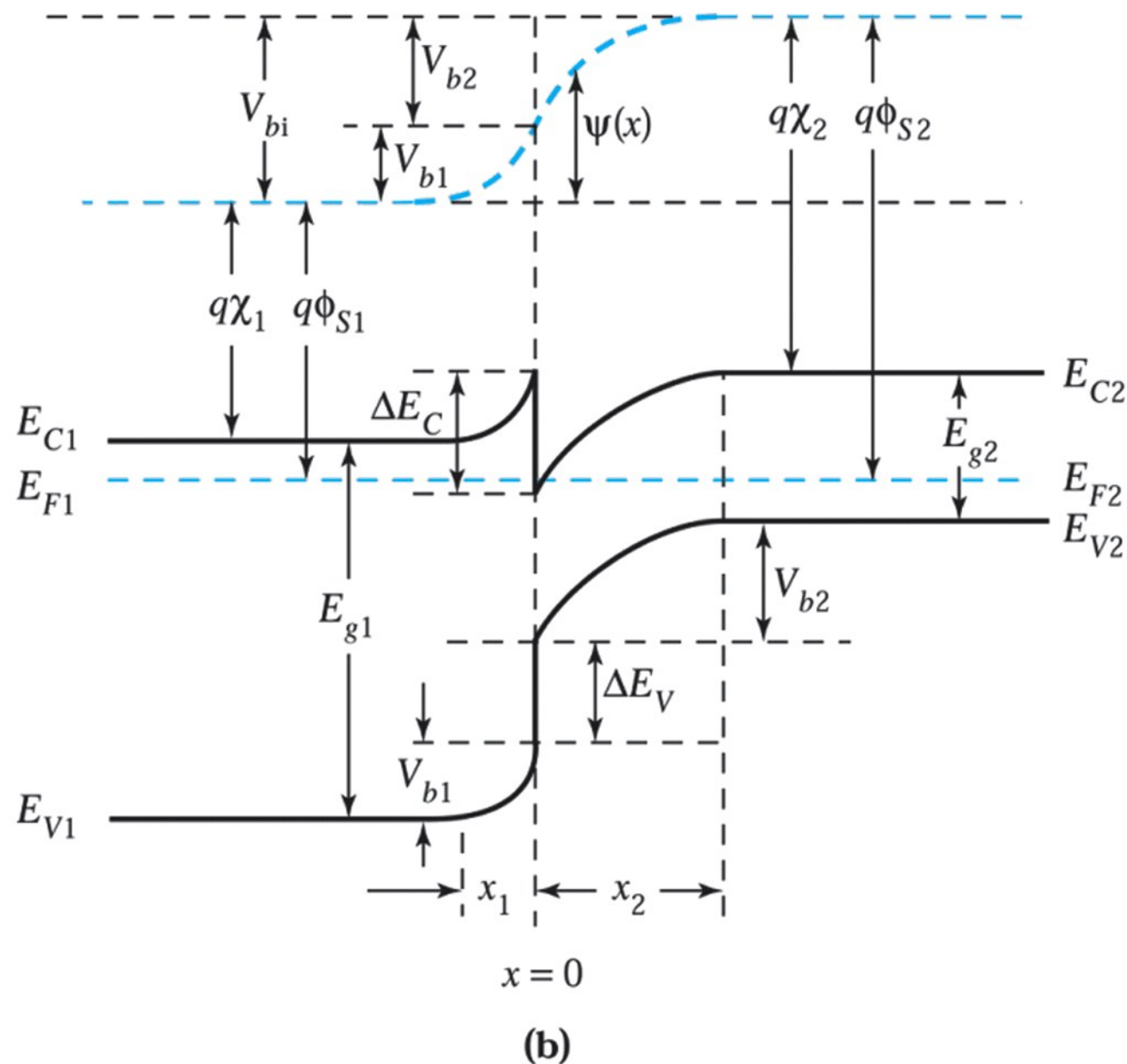


Figure 3.30a

© John Wiley & Sons, Inc. All rights reserved.



**Figure 3.30b**  
 © John Wiley & Sons, Inc. All rights reserved.